UPTEC X 05 054
DEC 2005
ISSN 1401-2138

GUNNAR DUNÉR

Molecular functionalization of QCM sensor surfaces

Master’s degree project

UPPSALA UNIVERSITET

Molecular Biotechnology Programme

Uppsala University School of Engineering

UPTEC X 05 054	**Date of issue 2005-12**

Author

Gunnar Dunér

Title (English)

Molecular functionalization of QCM sensor surfaces

Title (Swedish)

Abstract

An iniferter photopolymerization method was applied to QCM sensor surfaces to create 3D polymer matrices, detected by QCM and independently verified. The pK_a of an acidic gel was determined and BSA immobilized to acidic gels. Conclusions are that the pH of the protein buffer should not be too close to the pK_a of the matrix since it gives poor reproducibility, less electrostatic interaction with the protein and sub-optimal steric availability.

Keywords

Photopolymerization, iniferter, QCM, immobilization, MIP

Supervisors

M.Sc. Henrik Anderson
Attana Sensor Technologies, Stockholm, Sweden

Scientific reviewer

Ph.D. Peter Lindberg
Attana Sensor Technologies, Stockholm, Sweden

Project name	Sponsors Swedish Research Council
Language **English**	Security
ISSN 1401-2138	Classification
Supplementary bibliographical information	Pages **43**

Biology Education Centre Biomedical Center Husargatan 3 Uppsala
Box 592 S-75124 Uppsala Tel +46 (0)18 4710000 Fax +46 (0)18 555217

Molecular functionalization of QCM sensor surfaces

Gunnar Dunér

Sammanfattning

En biosensor består av två komponenter, en funktionell sensorkemi som reagerar med ämnet som ska analyseras, analyten, och en omvandlare som översätter den kemiska eller biokemiska signalen till en elektrisk signal. Den senare komponenten i detta fall använder sig av Quartz Crystal Microbalance som bygger på principen att kvartskristaller kan resonera då de utsätts för en oscillerande potential. Resonansfrekvensen minskar vid inbindning av analyter till ytan vilket relateras till den inbundna massan. Detta arbete har siktat på att utveckla den första komponenten, ytkemin, genom att polymerisera en tunn gel av akrylamid på sensorytan med hjälp av UV-ljus. Gelen kan funktionaliseras genom att skapa en tredimensionell matris till vilken man kan koppla en större mängd proteiner som ska fungera som igenkännande element för analyten vilket möjliggör större sensorvolym och ökad prestanda hos sensorn för existerande applikationer. Proteinkopplingen sker till karboxylatgrupper på inkorporerad akrylsyra i gelen. En helt ny tillämpning för sensorn kan också utvecklas genom att skapa gelbaserade artificiella antikroppar.

Resultaten visar att den fotopolymeriseringen fungerar som beläggningsmetod, att man kan uppnå reproducerbarhet i beläggningen och att protein kan fästas till gelen, om ändock i mindre omfattning än förväntat vilket innebär att kopplingsproceduren behöver optimeras.

Examensarbete 20 p i Molekylär bioteknikprogrammet

Uppsala universitet december 2005

Table of Contents

Table of Contents 1
Abbreviations 2
1 Introduction 3
1.1 Attana Sensor Technologies 3
1.2 Aim 3
2 Theory and Background 3
2.1 Concept of the Quartz Crystal Microbalance Biosensor 3
2.2 The iniferter technique 4
2.3 Immobilization of Proteins to a Carboxylated Polymer Matrix 6
2.4 Molecular Imprinted Polymers 7
2.5 White light interferometry 10
2.6 Ellipsometry 10
2.7 Electron spectroscopy for chemical analysis 11
3 Materials and Methods 11
3.1 Chemicals 11
3.2 Synthesis of Polystyrene-based Substrate Polymer PVBD 12
3.3 Synthesis of Polystyrene-based Polymer DC15 12
3.4 Coating of PVBC and PVBD 12
3.5 Polymerization conditions 12
3.6 Coupling Using EDC/NHS and Immobilization of Proteins 13
3.7 QCM-measurements 13
3.8 Ellipsometry 13
3.9 White light interferometry 13
3.10 Electron Spectroscopy for Chemical Analysis 13
3.11 NMR Spectroscopy 13
4 Results 14
4.1 Iniferter Polymer Synthesis 14
4.2 Iniferter Polymer Coating and Polymerization 15
4.2.1 Polymerization Using TD in a Two-Component Iniferter System 17
4.2.2 Polymerization Using Ethanol as a Solvent 19
4.2.3 Reproducibility of UV-photopolymerization 20
4.2.4 Hydrophilicity tests 20
4.3 Functionalized Polymers 21
4.3.1 QCM-measurements – pH Gradient 21
4.3.2 EDC/NHS Activation of Copolymer 23
5 Discussion 24
6 Conclusions 28
7 Future work 28
8 Acknowledgements 29
9 References 30

Abbreviations

DC15	PVBD-PVBC polymer in 1:5 relation
EDC	1-Ethyl-3-(3-dimethylaminopropyl)-carbodiimide
ELISA	Enzyme-Linked Immunosorbent Assay
ESCA	Electron Spectroscopy for Chemical Analysis
MIP	Molecular Imprinted Polymer
NaDC	Sodium Diethyldithiocarbamate
NHS	*N*-Hydroxysulfosuccinimide
PSI	Phase Shift Interference
PVBC	Polyvinylbenzyl Chloride
PVBD	Polyvinylbenzyl Diethyldithiocarbamate
QCM	Quartz Crystal Microbalance
RCA	Radio Corporation of America (method to remove organic contaminants from metal surfaces)
RIA	Radioimmunoassay
TD	Tetraethylthiuram Disulfide
VSI	Vertical Shift Interference

1 Introduction

1.1 Attana Sensor Technologies

Attana develops and markets biosensors using the quartz crystal microbalance technique along with sensor chips with various selective and metal coatings, e.g. for immobilization of biotinylated ligands and immobilization of proteins on carboxylated surfaces to name a couple. Since the company's foundation in July 2002, it has experienced a rapid development. Within 5 months the first prototype, Attana 80, was manufactured, and in March 2004 the first commercial one, Attana 100, was launched in Sweden and in the UK. The company is currently preparing for the launching of the next member of the Attana series, Attana 200, with new features like a two channel flow system and autosampling. Attana is involved in collaborations with leading universities and institutes both on surface chemistry, application development and instrumentation.

1.2 Aim

Attana has a long-term interest in developing new products and applications for existing products. As a part of this goal, the degree project focused on applying an exciting and very promising polymer coating method on the biosensor surface. The method should be controllable and give reproducibility, essential properties for the industrial coating of sensor chip surfaces. After establishing the coating procedure at a satisfactory level, there were two choices at hand to follow up. First, to create a 3D surface for the immobilization of proteins, second, to create MIPs for specific detection of proteins. During the course of the project, it was decided to focus on the first alternative.

2 Theory and Background

2.1 Concept of the Quartz Crystal Microbalance Biosensor

A biosensor consists of two components, a functional sensor chemistry that reacts on the analyte and a transducer that converts the chemical or biochemical signal to an electric signal. In the case of Attana's biosensor, the surface chemistry is the coating on the surface, e.g. streptavidin sensitized biotin layer, and the transducer is the quartz crystal which gives rise to change in resonant frequency, measured by a frequency counter.

The Quartz Crystal Microbalance (QCM) is a label free technique for mass detection. It relies on the piezo-electric effect, which is the phenomenon when a crystal vibrates mechanically if exposed to an oscillating electric potential and vice versa, it gives an electric signal if deformed. Each crystal has its own resonating frequency, which is dependent on the mass or thickness of the crystal. Thinner crystals resonate at higher frequencies and are consequently more sensitive, only the drawback is the more fragile crystal. For an AT-cut crystal the usual frequency region is around 10 MHz. When an analyte attaches to the surface, the mass of the crystal changes and so does its resonant frequency. Equation 2.1 is the Sauerbrey equation, which describes the relationship between the change in frequency and the change in adsorbed mass Equation 2.1. The Sauerbrey equation, where Δm (gcm^{-2}) is the adsorbed mass per unit area, Δf the frequency change, A the area of the gold (0,159 cm^2), f_0 the fundamental mode resonant frequency of the crystal (~10 MHz), ρ_q the density of quartz (2,648 gcm^{-3}) and μ_q the shear modulus of quartz (2,947·10^{11} $gcm^{-1}s^{-2}$).

$$\Delta m = \frac{-\Delta f A \left(\rho_q \mu_q\right)^{\frac{1}{2}}}{2 f_0^{\,2}} \qquad (2.1)$$

Equation 2.1. The Sauerbrey equation, where Δm (gcm^{-2}) is the adsorbed mass per unit area, Δf the frequency change, A the area of the gold (0,159 cm^2), f_0 the fundamental mode resonant frequency of the crystal (~10 MHz), ρ_q the density of quartz (2,648 gcm^{-3}) and μ_q the shear modulus of quartz (2,947·10^{11} $gcm^{-1}s^{-2}$).[1]

The QCM-technique is very sensitive and has the potential of pg detection limits[2]. As a sensitive detection technique, QCM has found applications for thin film deposition control, space system contamination studies and aerosol mass measurements[3]. More and more, QCM-devices have been used in analysis. The main advantage is the less complex instrumentation which makes it much less expensive.

2.2 The Iniferter Technique

Although positive results, major drawbacks with the method used previously in experiments performed by Karin Berggren[4] were the poor reproducibility and control over the

polymerization process, both regarding the thickness of the gel and the attachment to the underlying silicon dioxide surface. The physical methods below were all tested and evaluated by Berggren.

Physical
- Sandwiching or stamping
- Spin-coating
- Drop-coating

Chemical
- ATRP
- RAFT
- Iniferter

The defined problem is thus to use a method that fulfils a set of criteria for commercial application, among these are high reproducibility and the ability to control the polymerization process. Both ATRP[5], [6], RAFT[7], [8] and the iniferter method were considered, but it was decided that the most promising alternative the iniferter technique used by Nakayama & Matsuda[9], because of its simplicity. An iniferter system involves the initiation, chain transfer and termination of a radical polymerization by the same compound. The authors used the benzyl diethyldithiocarbamate group, which has been studied in detail by Otsu[10] and is photosensitive for UV-light at wavelengths 350-400 nm. When irradiated, the covalent bond between the carbon on the benzyl and the sulphur of the dithiocarbamate group breaks and a benzyl radical and a dithiocarbamate radical form. The process is reversible but is driven to dissociation by the UV-light. When vinyl monomers are introduced, such as acrylamide and acrylic acid, a chain transfer occurs and the elongation of a polymer chain starts. When shaded, the dithiocarbamate radical terminates the reaction by acting as a lid at the chain end, in other words the thickness of the polymer layer can be controlled by the irradiation time, which in principle can give a desirable thickness in the thin range wanted to make measurements with QCM meaningful. An overview of the reaction is seen in Figure 2.1 below. In the second step of initiation, a vinyl monomer is added to the benzyl carbon group. After initiation, chain elongation takes place by continuous addition of monomers. When shaded, the sulfur radical of the diethyldithiocarbamate group couples to the terminal monomer. Upon subsequent irradiation, the sulfur radical dissociates again).

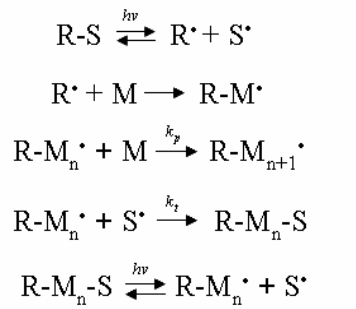

Figure 2.1. The reactions of the iniferter system. The radical reaction is initiated in a reversible process when the iniferter system is irradiated.

Using this technique Nakayama & Matsuda[9] achieved a linear frequency shift during 17 min of about 1400 Hz, hence this approach has the potential of extreme control. However, when working with protein MIPs a cross linker is needed which would introduce a non-linear growth behavior due to the addition of extra reactive groups in the cross linker. It is feasible that the polymerization is controllable during a short period.

2.3 Immobilization of Proteins to a Carboxylated Polymer Matrix

The hope is to apply the iniferter technique to create a 3D surface for the immobilization of proteins. This would increase the dynamic range and sensitivity in applications where large quantities of biomolecules are to be immobilized to detect very small analytes. Given that the loading capacity of proteins is in close parity with that of label-free mass detection instruments on the market today, it would be very interesting to see if a polymer matrix can exceed the sensitivity limits of these instruments.

In order to immobilize proteins to acrylic acid derived carboxylic groups, the EDC/NHS reaction is used.[11] Activation and coupling with EDC has many applications, for example attaching haptens to a carrier protein[12] or nucleic acids through 5' amino groups[13] and has been used in various biosensors[14, 15, 16]. The reaction is outlined in Figure 2.2. EDC binds to the carboxylate group of an acid and forms an unstable reactive o-acylisourea ester intermediate which is susceptible to hydrolysis. However, the ester can be stabilized through *N*-hydroxysulfosuccinimide to form a semi-stable amine-reactive NHS-ester. A protein with a free NH_2 group is subsequently coupled to form a stable peptide bond. If the primary ester is not stabilized, it can regenerate the carboxyl group.

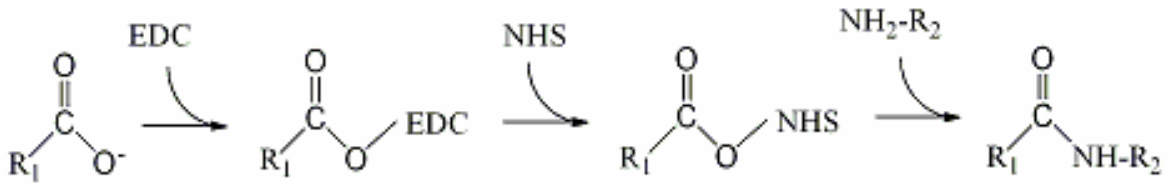

Figure 2.2. Reaction scheme for the creation of a stable peptide bond using the EDC/NHS system.

Proteins react with NHS-esters mainly through the α-amino group, the ε-amino group of lysine and the thiol group of cystein[11]. In order to facilitate the immobilization through electrostatic interaction, the protein buffer should have a pH which is below the isoelectric point of the protein. The degree of interaction thus depends on the sign of charge, charge density of the protein and the matrix, which is strongly dependent on its pKa. Hence, the prerequisite for good protein covalent coupling is to use a buffer with pH above the pKa of the matrix, but lower than the pI of the protein. It is the uncharged amino groups that couple covalently and thus this reaction is favored by a high pH. The interaction yield, the amount of immobilized material divided by the amount of electrostatically bound material, has its highest value at large pH, however the degree of electrostatic interaction is determinant for the absolute amount of immobilized material and is found not to close to the proteins pI [11]. Another reason for using a buffer with pH well above the pKa is to avoid poor reproducibility, since the charge of the matrix might fluctuate heavily around its pKa. It should not be too high of course, since as much electrostatic interaction as possible still preferred. For easy coupling, the pI of the protein should not be too close to the pKa of the matrix.

2.4 Molecular Imprinted Polymers

Antibodies are today widely used as a versatile tool within life sciences and clinical medicine. They are for example used in QCM for selectivity. Monoclonal antibodies can be produced by the fusing of immunized B-cells from mice with a mutant myeloma line. The fused hybridoma cells can be selected for and have the capacity to grow in large numbers. Cell clones producing antibodies for the specific antigen are screened using enzyme-linked immunosorbent assay (ELISA) or radioimmunoassay (RIA). The procedure is time consuming and costly, only selection for hybridized cells can longer for weeks and it is not free of charge to house animals. On top of this there is the ethical problem of sacrificing animals. [17]

A novel method for the specific detection of antigens should be faster, more cost effective and not have to deal with ethical issues as today. One technique which could possibly meet all these criteria would be that of molecular imprinted materials or molecular

imprinted polymers (MIP) for proteins. The concept is explained by Figure 2.3 below. Monomers in solution polymerize to form a pocket around a protein. The protein is subsequently eluted by a detergent such as SDS. Left is the imprinted polymer which now has binding sites for the very same protein.

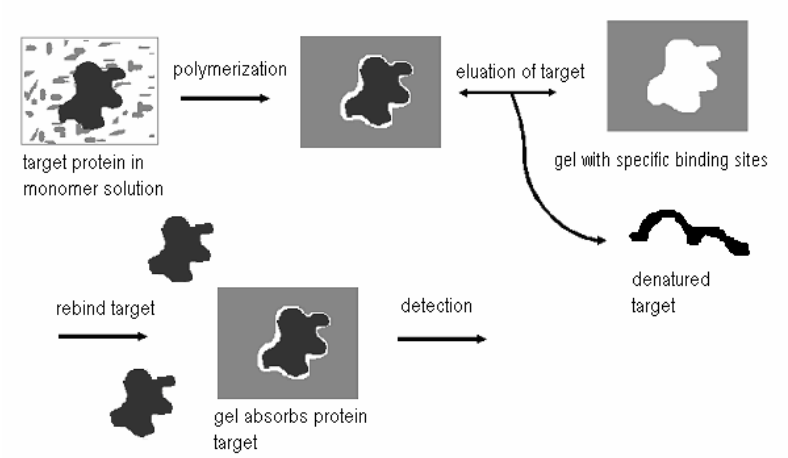

Figure 2.3. The MIP concept for proteins. Monomers in a protein solution polymerize to form a specific pocket around the protein. The protein can be eluted by a detergent such as SDS to leave the pocket behind. When the very same protein is introduced again it can rebind to the pocket. (Illustration used and modified with permission from Karin Berggren[4])

Usually, the molecular imprinting technology relies on the interactions of the imprinted molecule to so-called functional monomers, which are coupled to a polymer matrix. Modes of interactions include ionic interactions, hydrogen bonds, π-π-interactions and hydrophobic interactions. Polymer matrices are often polyacrylate-/acrylamide- or polystyrene-based. Functional monomers comprise various carboxylic acids, sulphonic acids and heteroaromatic weak bases.

The use of molecular imprinted polymers obviously concern areas where molecular binding is of interest. Among the practical applications can be seen tailor-made separation materials, antibody and receptor binding site mimics in recognition and assay systems, catalytic enzyme-mimics and recognition elements in biosensors. Table 2.1 summarizes main applications and gives examples of imprinted compounds. There is a broad spectrum of benefits when using MIPs for antibody binding mimics. Compared to conventional antibodies a MIP is easy to prepare, stable, it can withstand high temperature, pressure, extreme pH-values and organic solvents. It is possible to induce MIPs against immunosuppressive agents and they have possibly better recognition of haptens. They are a low-cost alternative to traditional antibodies. In addition, MIPs can function as alternative to hard-to-isolate

receptors. General disadvantages include the substantial amount of print molecule needed and the low capacity, 0.01-0.1 mass percent imprint molecule/polymer.

Table 2.1. Main applications of MIP. (See ref. 18 for details.)

Application	Method	Imprinted Compound
Separation	Column chromatography	Chiral compound
	TLC	Amino acid derivative
Antibody and receptor binding mimics	Immunoassays	Drugs, for example bronchodilator theophylline
Catalysis and artificial enzymes	Polymer imprinted for transition state analogs	E.g. use of transition state analogs in MIP
Biosensors	Fiber-optics	Fluorescently-labeled amino acid

The predominating solvents used have been organic because of the solubility nature of the cross-linkers. However, when running the system in aqueous solutions, it often still recognizes the imprinted compound. In any case, when imprinting proteins organic solvents cannot be used for natural reasons. [18]

In preliminary experiments work by *Liao et. al*[19] it was shown that gel column beds of polyacrylamide prepared in the presence of cytochrome C, hemoglobin and transferrin selectively adsorbed the respective protein. The authors concluded that the beds exhibited an unusually high specificity which could be utilized in the extraction and removal of target substances. In a later paper *Hjertén et al.*[20] extended the results to HGF, ribonuclease and horse myoglobin, suggesting that the selectivity of the polyacrylamide gel could be applicable to a great number of proteins or even generally applicable. Moreover, the gel columns have the potential to be highly specific since a bed column could discriminate between horse myoglobin and whale myoglobin. The question addresses whether the proteins are covalently bond to the gel matrix upon radical polymerization. Some support that this is not the case is presented. What is more, the authors hypothesize that the selective binding of the proteins is due to a great number of weakly interacting bonds such as hydrogen bonds, induced dipoles in close proximity to the protein, which is assumed to be the result when polymerizing in protein solution. Hence a protein with larger molecular weight should bind more strongly to the matrix than a smaller macromolecule and accordingly, the smaller protein insulin (MW 5 700) showed less adsorption to a gel prepared for insulin. However, the authors do not exclude any other binding mechanism.

2.5 White Light Interferometry

The white light interferometer is an optical profiler and can give the smoothness of a surface. A rough surface can cause problems for the QCM measurements and the Sauerbrey equation may not be applicable. Therefore it is important to decide the roughness of the surface. The profiler can measure in two different modes, Vertical Shift Interference (VSI) or Phase Shift Interference (PSI). The former can handle topographies up to the mm regime while the upper limit for the latter is 150 nm. For spin coated samples the PSI mode has been used. The PSI mode utilizes the phase shift between light reflected from the sample and a reference beam. As a piezoelectric transducer translates the reference very short distances, the instrument records and integrates the intensity patterns on the sample which results in wave front data and imaging.[21]

2.6 Ellipsometry

This technique is an excellent tool for measuring thin-film thicknesses. In this work it is used to see whether thin enough films can be achieved or not for QCM application. Light that is incident on a surface can be decomposed into a p-component parallel to the plane of incidence and to an s-component perpendicular to the plane of incident. It is the ratio of these components after reflection that is measured. Usually this relationship can be expressed as:

$$\rho = \frac{R_p}{R_s} = \tan\Psi e^{i\Delta} \qquad (2.2)$$

where $\tan\Psi$ corresponds to the amplitude change after reflection and Δ to the phase shift. Since the ratios of two parameters are measured, the accuracy is very high, Ångström resolution can be achieved. In addition ellipsometry has the advantage of being non-destructive.

Ellipsometry is a model-dependent technique. A theoretical model has to be created that describes the sample in terms of refractive index and/or thicknesses of layers. The experimental data from the sample is then fitted to the theoretical model. The χ^2 parameter is used to evaluate the fit. The better the fit, the smaller the χ^2-value and the closer the sample corresponds to the theoretical model. How good a fitting can be is related to the number of layers and thereby the number of parameters. The fitting is an iterative process described by Figure 2.4. If the results are not to satisfaction, the parameters in the model or the model itself have to be changed.[22]

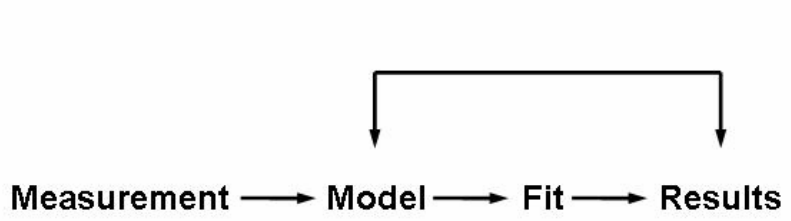

Figure 2.4. The ellipsometry process. A model is created of the thin film which is fitted to the measurements. The model is updated by using the resulting parameters from the fitting.

2.7 Electron spectroscopy for chemical analysis

Electron spectroscopy for chemical analysis (ESCA) is a very powerful tool for surface chemistry analysis and in this work is has been used to verify surface coatings, both the pureness of the substrate polymer PVBD and presence of acrylamide. The principle of ESCA is as follows, an electron cannon shoots electrons at 16000 V, 500 mA into a rotating metal disc of aluminium in ultra-high vacuum. X-rays emanate from the disc and are monochromated when reflected on quartz crystals; the reflected light has now energy of 1486.7 eV. The sample is hit by Al K α-photons which are capable of knocking out electrons of various energy levels in the sample according to

$$h\upsilon = E_B + E_{kin} + \phi_{sp} \qquad (2.3)$$

The electrons enter a lens and are decelerated and focused into a small slit. After passing the slit the electrons are bent in an electrostatic field according to their kinetic energy and hit the detector. A CCD-camera detects the flashes from the detector and each hit is registered and counted. Software converts the counts to a spectrogram which show the electron counts as a function of binding energy. Each element has its fingerprint. Of course, nearby elements in molecules affect the binding energy, giving rise to a shift in the spectrogram. When identifying compounds, e.g. polymers, references are used.

3 Materials and Methods

3.1 Chemicals

Poly(vinylbenzyl chloride), Sodium Diethyldithiocarbamatetrihydrate were purchased from Sigma. All solvents and organic liquids were from SDS. Acrylamide (99,9 %) was purchased from Bio-Rad, acrylic acid from Fluka, ethanol from Kemetyl. For RCA-washing 1 eq. of 28

% ammonia solution, 1 eq. 7 eqs. of water and 1 eq. of 31% hydroperoxide solution were used.

3.2 Synthesis of Polystyrene-based Substrate Polymer PVBD

The chemicals PVBC (0.9995 g) and NaDC (4.9999 g) were mixed in a round flask. 55 ml THF was added and the mixture was stirred over night. After evaporation of THF the contents were dissolved in chloroform in an extraction flask. Deionized water was added on top and the extraction flask was heavily shaken for 50 s. This was repeated twice. The round flask was weighed before and after extraction.

3.3 Synthesis of Polystyrene-based Polymer DC15

PVBC (1.0012 g) and NaDC (0.2980 g) were mixed in a 100 ml round flask. 50 ml THF was added and the mixture was stirred over night. The solvent was evaporated and the contents were rinsed twice with deionized water in order to remove unreacted NaDC. The product was subsequently dried in methanol. The product was further purified by extraction in 75 ml chloroform. Deionized water was added and the extraction flask was heavily shaken for 50 s. This was repeated twice.

3.4 Coating of PVBC and PVBD

Crystals were washed in ethanol 99.5 % and dried by a nitrogen gas flow prior to coating. The coatings of the crystals were either spin coating or drop-coating. In the latter case the plastic polymer was dissolved in toluene and three drops of solvent were dropped on the gold surface. The sensor chips were subsequently dried at a moderate flow of nitrogen gas. Three droplets were applied to spin-coated crystals and were immediately spun at 2000 rpm for 60 s. Gold samples prepared for ESCA were RCA treated after washing in ultrasonic bath in ethanol for 5 min in order to remove organic contaminations.

3.5 Polymerization Conditions

Before use, all glassware used were thoroughly washed and dried in oven at 110°C. Acrylamide was weighed and put into a round flask. Water or ethanol was subsequently added. In the case of copolymerization, acrylic acid was added to the solvents. The solution was degassed using vacuum from the tap for at least 10 min or until all bubbles were removed and the bottom of the flask was cold. To further limit the amount of dissolved oxygen in the solution, a nitrogen atmosphere was applied. Until use, the round flask was sealed with parafilm.

The coated crystals were mounted into a Pyrex glass tube, which has a wavelength cut-off of 300 nm. The tube was sealed at both ends except for an opening into which nitrogen was flowed onto the monomer solution. The monomer solution was poured into the tube. The UV-lamp used was s broad spectrum mercury lamp of 400 W at a distant of 8,5 cm from samples. The lamp was cooled by a water flow. The samples were irradiated for 60-90 min.

For the immobilization of proteins samples were incubated >72 h in a 1 M acrylamide, 0.5 M acrylic acid monomer solution. Water coolant was set on a minimal flow to allow a better heat-up of the UV-lamp. Samples were irradiated for 60 min.

3.6 Coupling Using EDC/NHS and Immobilization of Proteins

See Appendix C for details.

3.7 QCM-measurements

The measurements were performed in dry conditions except otherwise stated. Before measuring, the samples were washed in solvent, dried by an applied nitrogen gas-flow until all solvent had evaporated. Samples were mounted in the Attana 100 plug-and-play chips and inserted into the instrument. Before measuring, care was taken that the sensor surface and chips were dry. Measuring was performed for at least 60s.

3.8 Ellipsometry

Ellipsometry measurements were performed with a Jobin Yvon spectroscopic ellipsometer. Angle of incidence was 65° and the Cauchy-absorbent parametrization was used for curve-fitting.

3.9 White light interferometry

Measurements were done with a WYKO NT2000 white light interferometer in the PSI mode.

3.10 Electron Spectroscopy for Chemical Analysis

Measurements were done with the ESCA 300 from SCIENTA. Samples were positioned at a 90° angle to the detector, unless otherwise stated.

3.11 NMR Spectroscopy

^{1}H NMR spectra were recorded using a Bruker AC200 spectrometer at 298 K.

4 Results

4.1 Iniferter Polymer Synthesis

In order to create the active iniferter substrate polymer PVBD, PVBC reacted with NaDC. Maximum yield of PVBD was 1.7374 g. The round flask measured 1,579 g after evaporation giving a yield of 91 %. This figure could be higher but is acceptable since some material was lost during handling. Standard confirmation of the product was performed by looking at it in NMR. Figure 4.1 shows the ^{1}H NMR-spectrum of PVBD. The area proportions are directly related to the proportions of different groups of hydrogens in the polymer, which can be found at different chemical shifts. The ratios of the integrals of the three curves are 4:6:9 (100.00:140.72:225.70), which is expected. The spectrum confirms the product PVBD.

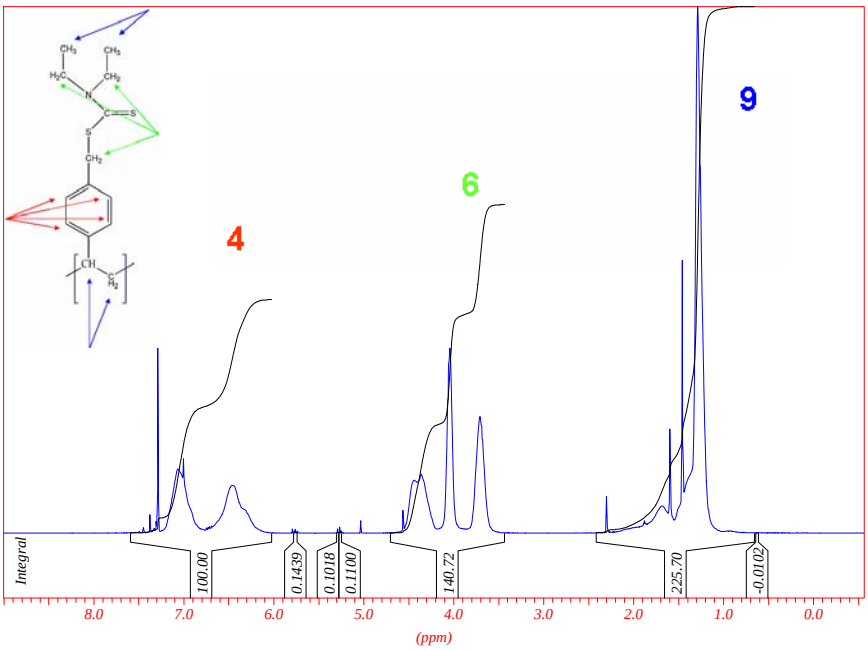

Figure 4.1. NMR-spectrum of PVBD. The ratios of the integrals of the three curves are 4:6:9 and corresponds to the number of hydrogen atoms in the polymer.

A modified surface, DC15, was also produced with 5-fold less density of iniferter groups, with the hope of avoiding cross-linking of neighbouring iniferter-sites. Table 4.1 shows the yield of the product DC15 is close to 100 %.

Table 4.1. The yield of the substrate polymer DC15 is shown.

	mass / g	yield / g	yield / %
Round flask	63,6551	-	-
after evaporating	64,8983	1,2432	108,3
90 min in 40°C and vacuum	64,8399	1,1848	103,2
130 min in 40°C and vacuum	64,8096	1,1545	100,6
vacuum pump 60 min	64,8068	1,1517	100,4

This is to be expected since the number of PVBC is smaller than that of NaDC. A slightly too large yield is interpreted as not all solvent has evaporated and is still trapped in the polymer. See Appendix for the NMR-spectrum of DC15. The ratios of the peaks are 20:13.3:21.7 (817311:543040:886102), indicating a slighter less prevalence of PVBD in the polymer than 1/5.

4.2 Iniferter Polymer Coating and Polymerization

In order to confirm good enough smoothness of surfaces for QCM application, an optical profiler was used. See the Appendix A for a spin-coated PVBD surface profile on a gold substrate where the solvent used was THF and the measuring mode was PSI. Red color denotes higher areas and blue lower areas. The red horizontal and blue vertical lines are profiles that are also depicted in Appendix A and show that the roughness is about 5 nm, although holes are seen in the structure. These are detected by ordinary microscope as well. The holes are not detectable in visual microscope when changing solvent to toluene.To assure thin enough substrate polymer layers of PVBD for QCM application, ellipsometry was used to measure film thicknesses. Table 4.2 shows the results of ellipsometry measurements of spin-coated PVBD, 10mg/ml in toluene, 2000 rpm for 60 s. The initial value of the refractive index was set to 1.59. χ^2-values are generally lower than 0.3 and not shown.

Table 4.2. Thickness determination of spin-coated PVBD samples by means of ellipsometry using a concentration of 10 mg/ml of PVBD in toluene. Samples are spin-coated at 2000 rpm for 60 s.

Sample	Edge Thickness / Å	Center Thickness / Å
1	391	319
2	304	238
3	314	304
4	385	337
5	392	334
6	-	368
Average	357	317
SD	44	44

Drop-coating is easier to apply than spin-coating since crystals don't have to be mounted into a frame when measuring in QCM. The reproducability is though seemingly a bit worse. However, if the drop is properly applied, drop-coated samples are no worse than spin-coated for application since the surface profiles show a roughness in the similar range (~5 and 10 nm respectively). See Appendix A for an optical profile of a spin-coated sample. Drop-coated sample is not shown.

Table 4.3 shows the frequency shift of some samples when PVBD has been physisorbed.

Table 4.3. QCM-measurements on drop-coated samples. Average mass change is 3592 ng with a standard deviation of 803ng.

Sample	Shift / -Hz	Mass Change / ng
1	6648	4669
2	5992	4208
3	3971	2789
4	4469	3139
5	4493	3155
Average	5115	3592
SD	1144	803

In order to verify the chemical composition of surface layers, ESCA has been applied to detect the presence of acrylamide and to independently verify the product PVBD. Figure 4.2 and Figure 4.3 show the results from measurements with the ESCA 300. The peaks show the 1s carbon. [23,24]. It is clear that there is a difference between the UV-irradiated sample in acrylamide monomer solution and the PVBD surface. In the former is a minor peak shifted to higher binding energy. It stems from oxidized doubly-bound carbon, only present in acrylamide but not in PVBD. It is a strong indication that acrylamide is attached to the surface. The UV-irradiated sample has been extensively washed after irradiation.

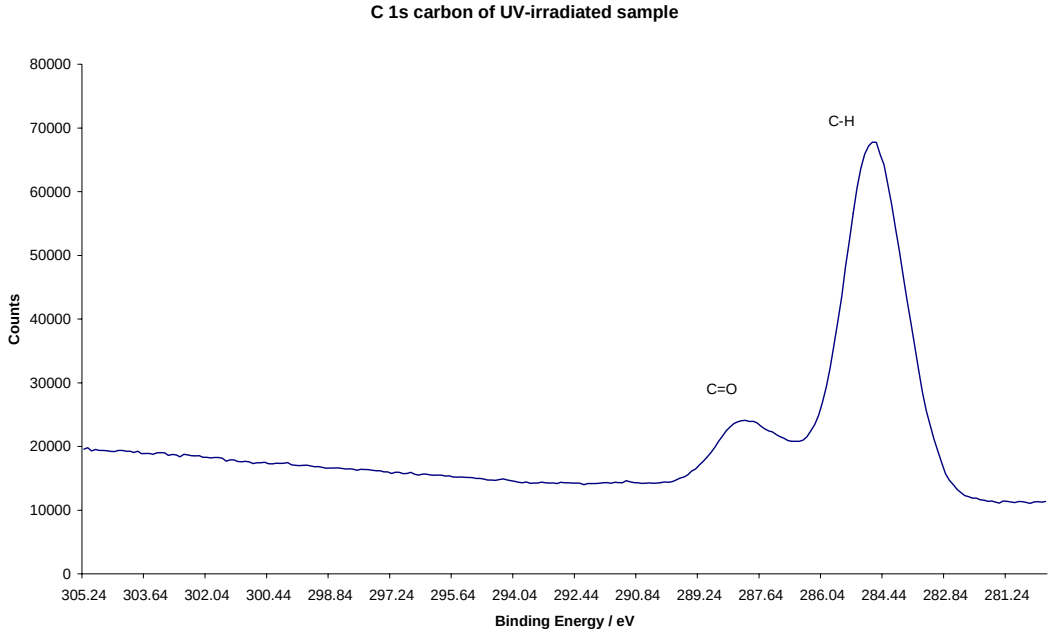

Figure 4.2. Spectrogram of the C 1s carbon of a UV radiated sample. A small part of double-bound oxidized carbon constitutes the 1s peak.

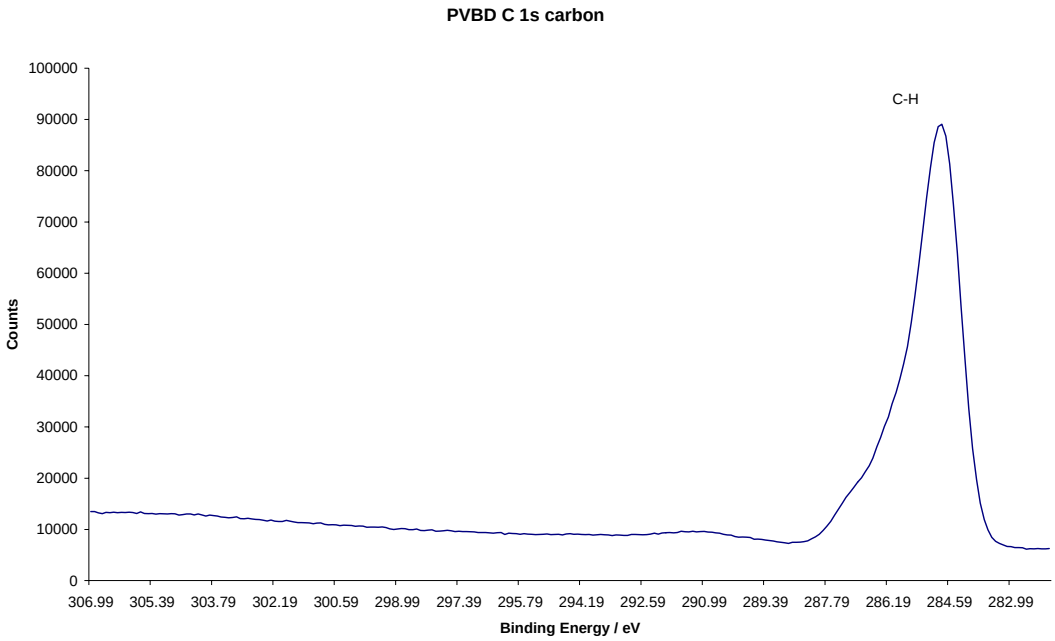

Figure 4.3. Spectrogram of the C 1s carbon of a PVBD sample. No double-bound oxidized carbon is visible.

4.2.1 Polymerization Using TD in a Two-Component Iniferter System

TD can increase efficiency of photopolymerization, especially where unwanted cross-linking reactions are expected[10]. Table 4.4 and Figure 4.4 show the frequencies and shifts for DC15 and the non-irradiated control in monomer solution. After 268 min a shift of 835 Hz is seen. The controls were incubated in monomer solution but not UV-irradiated. At each measuring point, the sample and the control have been removed from monomer solution, dried in nitrogen gas flow and measured in an external chip.

Table 4.4. Frequencies and shifts for DC15 and the non-irradiated control in monomer solution containing TD.

UV / min	DC15 / Hz	DC15 Control / Hz	Adjusted Control / Hz	Shift / Hz	Mass Change / ng
0	9997316	9993654	9997316	0	0
86	9997299	9993658	9997320	-21	15
268	9996494	9993667	9997329	-835	586

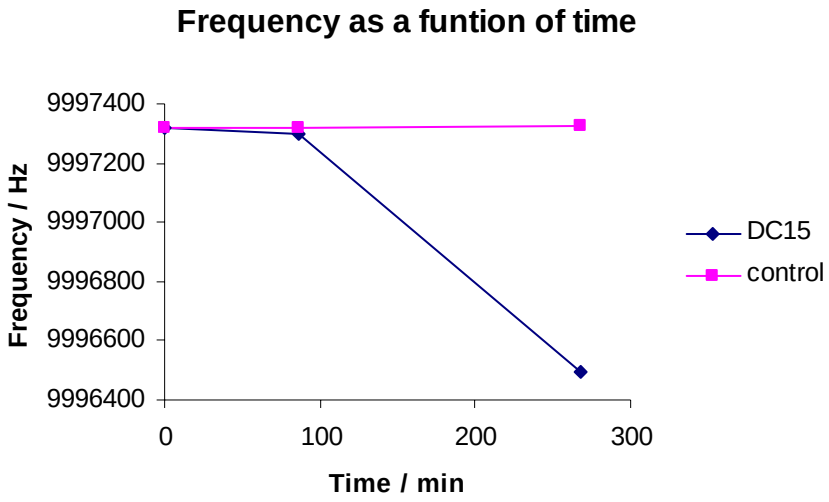

Figure 4.4. Visualization of Table 4.4. Between 86 and 268 min there is a major shift in frequency.

Table 4.5 and Figure 4.5 show the frequencies and shifts for PVBD and the non-irradiated control in monomer solution. After 268 min a shift of 660 Hz is seen, if the control is subtracted from the sample. At each measuring point, the sample and the control have been removed from monomer solution, dried in nitrogen gas flow and measured in an external chip.

Table 4.5. Frequencies and shifts for PVBD and the non-irradiated control in monomer solution.

UV / min	PVBD / Hz	PVBD Control / Hz	Adjusted Control / Hz	Shift / Hz	Mass Change / ng
0	10000915	9995260	10000915	0	0
86	10000943	9995480	10001135	-192	135
268	10000590	9995595	10001250	-660	464

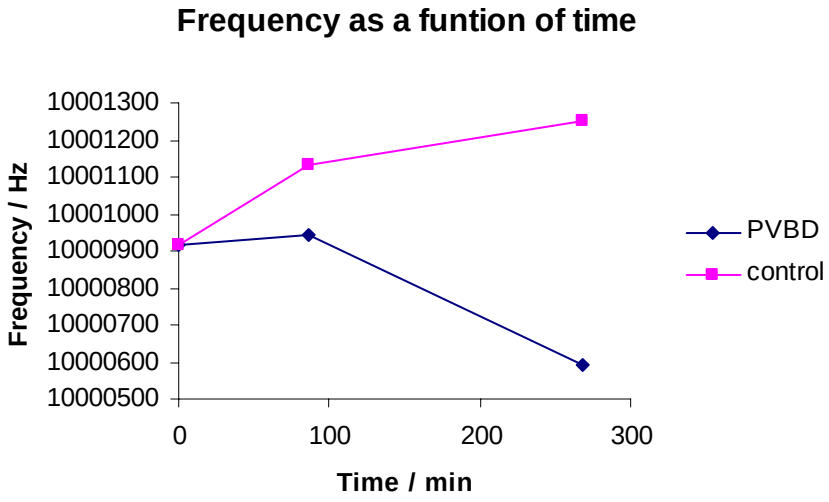

Figure 4.5. Visualization of Table 4.5. Between 86 and 268 min there is a major shift in frequency.

4.2.2 Polymerization Using Ethanol as a Solvent

In order to investigate whether the great shift came from the presence of TD or ethanol a control experiment was conducted with no TD present in the monomer solution. Table 4.6 and Figure 4.6 show the frequencies and shifts for DC15, Table 4.7 and Figure 4.7 for PVBD. For the case of DC15, there is a shift of ca 2200 Hz between 0 and 135 min and an additional shift of ca 1700 Hz after another 60 min. For PVBD such a largeshift as ~5000 Hz is detected after 195 min of UV irradiation.

Table 4.6. Frequencies and shifts for DC15 and the non-irradiated control in monomer solution.

UV / min	DC15 / Hz	DC15 Control / Hz	Adjusted Control / Hz	Shift / Hz	Mass Change / ng
0	9996653	9999674	9996653	0	0
135	9994448	9999671	9996650	-2202	1564
195	9992747	9999684	9996663	-3916	2750

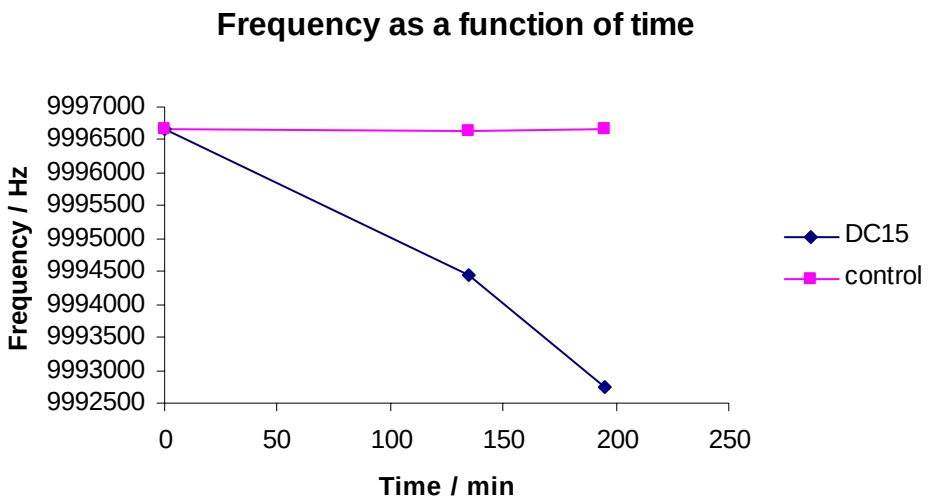

Figure 4.6. Visualization of Table 4.6.

Table 4.7. Frequencies and shifts for PVBD and the non-irradiated control in monomer solution.

UV / min	PVBD / Hz	PVBD Control / Hz	Adjusted Control / Hz	Shift / Hz	Mass Change / ng
0	9997528	9995628	9997528	0	0
135	9995963	9995624	9997524	-1561	1096
195	9992480	9995625	9997525	-5045	3543

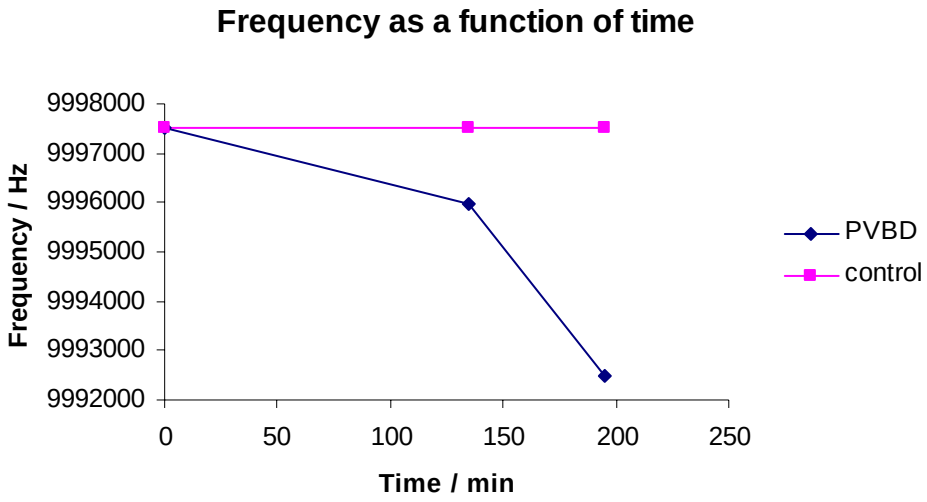

Figure 4.7. Visualization of Table 4.7 between 0 and 135 min there is a shift of ca 1600 Hz and an additional shift of ca 4500 Hz after another 60 min.

4.2.3 Reproducibility of UV-photopolymerization

The photopolymerization is shown to give reproducibility in Table 4.8, which show the frequency shifts for the copolymerization with 33% acylic acid for a irradiation time of 60 min. The standard deviation is 6.1 % of the average. Immediately after polymerization, the samples have been washed in deionized water, dried on the surface and measured.

Table 4.8. The spread in frequency shift of four samples produced at the same time.

Sample	Before / Hz	After / Hz	Shift / -Hz	Mass Change / ng
1	9999095	9997485	-1610	1130
2	9992159	9990566	-1593	1119
3	9996226	9994436	-1790	1257
4	10000058	9998291	-1768	1242
Average			-1690	1187
SD			103	72

4.2.4 Hydrophilicity tests

For the verification of the photopolymerization, hydrophilicity test was used. 10 µl of deionized water was applied to the washed surfaces after exposure to UV-light. The surfaces of the samples which had undergone successful polymerization showed increased hydrophilicity, the water droplet spread out over the whole surface. When removing the droplet, a thin water film was left. Figure 4.8 exemplifies with a typical result. The right sample has been UV-exposed where the edges of the water drop is easily seen. The left negative control shows a greater inclination of the edges.

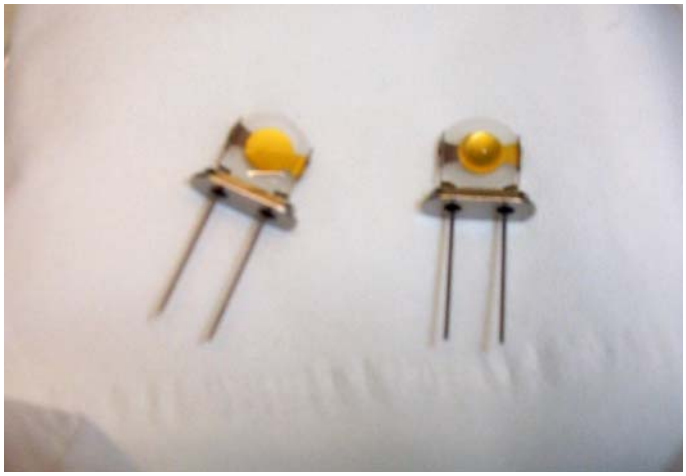

Figure 4.8. Hydrophilicity test as verification of successful photopolymerization. Left, UV-exposed PVBD-sample, the water drop adheres to the whole surface; right, negative control, incubated in monomer solution but no UV-exposure.

4.3 Functionalized Polymers

4.3.1 QCM-measurements – pH Gradient

Figure 4.9 shows the reproducible expansion and retraction of a p(Am-co-Aa) copolymer with 10% acrylic acid. An acrylamide reference is also shown.

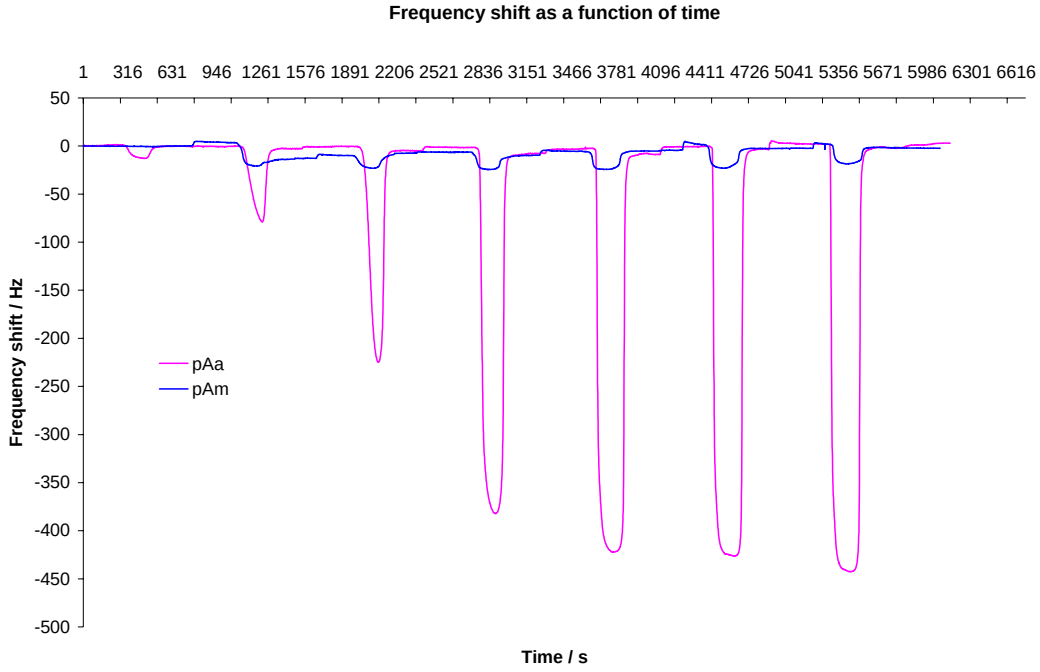

Figure 4.9. Frequency shift measurements with the Attana 100 biosensor. The figure shows responses of a copolymer, p(Am-co-Aa) with 10% acrylic acid, pink, and a pure pAm polymer, blue, to injections of PBS buffer with pH 3-9 from the left to the right. Running buffer had pH 2.

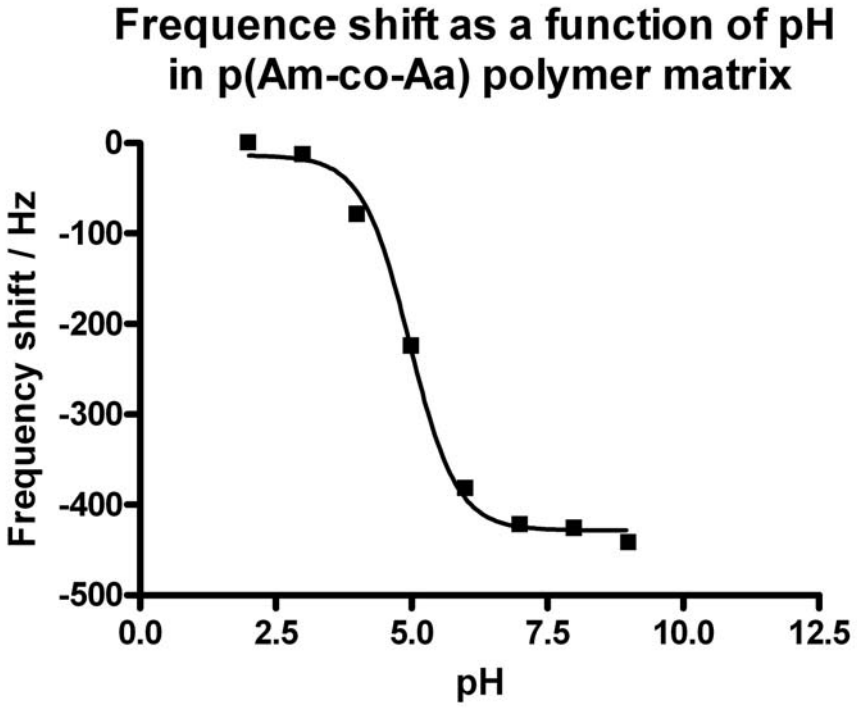

Figure 4.10. Maximum peak-shifts from pAa in Figure 4.9 are plotted against pH of the injections. Curve fitting using non-linear regression is shown. An extra measuring point is introduced, 0 Hz shift at pH 2 which was the running buffer.

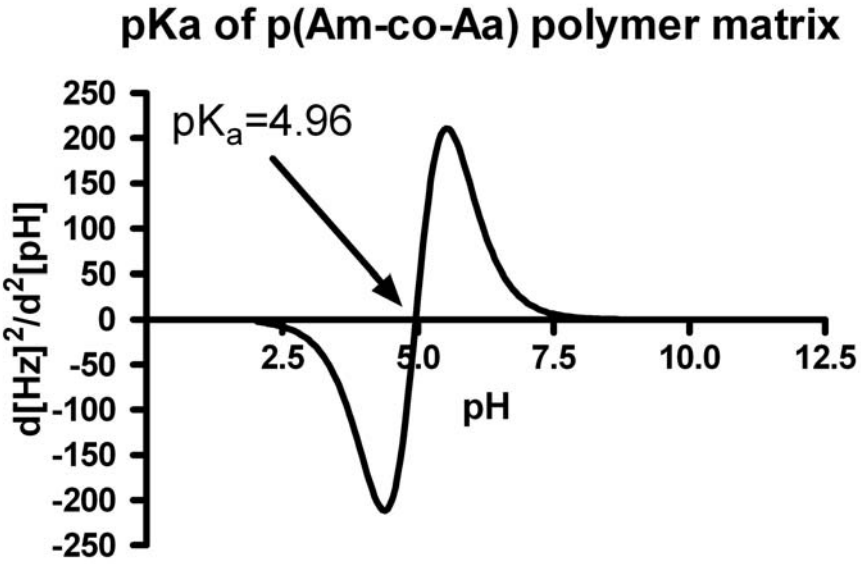

Figure 4.11. The second derivative of Figure 4.10 is shown. The pK_a is found where the curve changes sign, and is calculated to 4.96.

In Figure 4.9, an increase in pH expands the copolymer since the carboxyl-groups are deprotonated. The higher the pH, the larger the expansion until the gel is saturated with COO^-. The increase in frequency shift is due to the extra amount of water that resonates within the gel. The pure acrylamide polymer only shows little background. Buffer has been adjusted

with HCl and NaOH. Figure 4.10 and Figure 4.11 show the curve fitting of peak values in Figure 4.9 and the second derivative of Figure 4.10 respectively. From the fit it is possible to deduce the pK_a of the copolymer (see Figure 4.11). The pK_a is important for the choice of protein to immobilize and consequently the pH of the protein buffer.

4.3.2 EDC/NHS Activation of Copolymer

Figure 4.12 shows EDC/NHS activation of a 33% acrylic acid-acrylamide copolymer, response to successive injections of BSA and deactivation of activated carboxylate groups with ethanolamine. Figure 4.13 shows antibody detection of BSA.

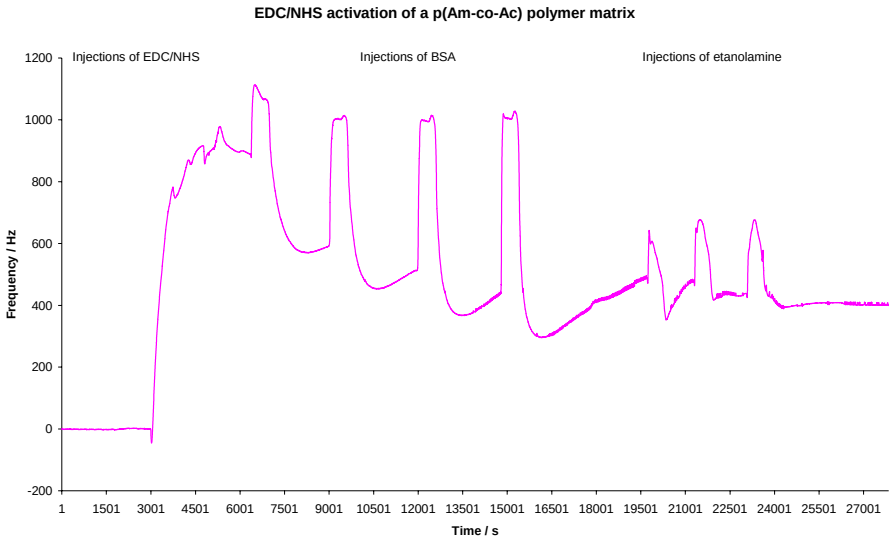

Figure 4.12. EDC/NHS coupling to carboxylate groups in copolymer of acrylamide and acrylic acid with 33% of the acid. Etanolamine isused to deactivate activated carboxylate groups.

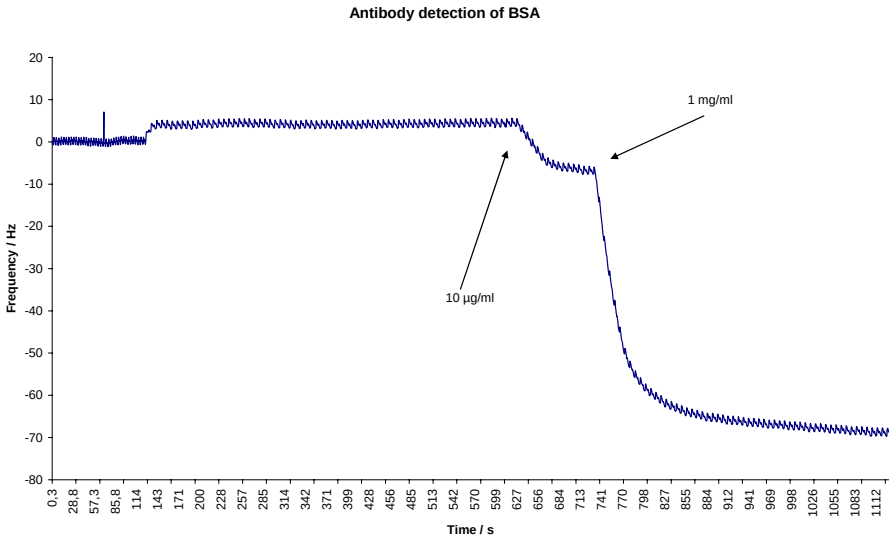

Figure 4.13. Antibody detection of BSA.

5 Discussion

The aim of this project was to apply a polymer coating method that could give thin enough and reproducible polymer layers for QCM application. If this goal was reached, a number of possibilities could be followed up, among them the immobilization of proteins to the polymer matrix for the cration of a 3D surface for increased sensitivity and the MIP project which would aim at creating specific binding of proteins to an acrylamide based polymer gel. However, the prerequisite for these projects was to have a reproducible polymer coating method. The path chosen was to make use of the iniferter technique. In order to reach this goal some problems had to be solved. First there was the need to produce a substrate carrying the active iniferter groups that could respond to UV-light. It was decided to make use of the polystyrene based polymer PVBC and to couple covalently the active dithiocarbamate groups to PVBC since polystyrene would adsorb to gold by physisorption. The polymer product PVBD was synthesized and purified by chloroform extraction.

The wanted product had to be verified. By using NMR spectroscopy and ESCA the PVBD substrate polymer was verified. The area relations of the NMR spectrogram can explain the different hydrogens in the substrate polymer and the chemical shifts are in accordance with what can be found in the litterature[25, 26]. In addition the ESCA spectrograms (see Appendix) show that the current method of synthesizing and purifying PVBD from PVBC is seemingly 100% efficient.

In possession of a clean product, there were two options at hand to coat the gold surface of the crystals with the substrate polymer, spin-coating or drop-coating. The former alternative was presumed to give more smoothness of the surface and thinner layers, which is good for QCM application since every chip has a limited loading capacity. The latter was more attractive in the practical laboratory work perspective since crystals are already attached to the conducting frameused in the Attana instruments. The different coating modes were evaluated with regard to roughness since it is important to have a smooth surface since the Sauerbrey equation holds for smooth surfaces. It turned out that the smothness or roughness was in the same range for both methods. In addition, no problems with QCM measurements were observed because of the presumably thicker layer of substrate polymer when drop-coating at concentrations ≤13 mg/ml. With this information at hand it was decided to continue with drop-coating. Unexpectedly, it was discovered by optical profiling that when THF was used as a solvent, holes in the polymer substrate layer appeared. Changing solvent to toluene dimnished this effect as verified by optical microscopy. Probably this unwanted effect was due to evaporation properties of the solvent. SEM pictures (data not shown) confirmed the

presence of the holes. With radii > 6 nm the holes are large enough for hemoglobin to fill. It is poosible though that a photopolymerized gel layer can become thick enough to hinder proteins to diffuse into these cavities. In any case, from Table 4.2 and
Table 4.3 it seems that spin coating can give higher reproducability in the substrate polymer thickness, however a sufficient thin and smooth layer can be achieved by drop-coating shown by experience.

Having a clean substrate polymer and a coating method that worked, next step was to test the iniferter system in acrylamide monomer solution. ESCA was used to detect the presence of acrylamide on the PVBD substrate on the gold surface. From Figure 4.2 and Figure 4.3 a clear difference can be seen in the C 1s peaks of the two spectrograms. On the UV-irradiated sample there is a smaller peak to the left of the larger peak. This is because of double-bound oxidized carbon[24], only found in acrylamide. However, the surface did not show the hydrophilic properties expected. It is possible the polymerization had not gone far enough, because it seems unlikely that acrylamide monomers should attach to the surface after very extensive washing. With ESCA, there is no way to discriminate between monomers and polymers of acrylamide. This result led to the optimizing of photopolymerization conditions. Results were measured by QCM and verfied by an independent method, a simple hydrophilicity test. During the course of optimization, there seemed to be a lag-phase in the system. Whether this is a true property by the iniferter system or an artificial effect is unclear. It may be because of insufficient heating of the UV-lamp for example. Nevertheless it was very difficult to reproduce increased hydrophilicity after UV-irradiation. The following parameters were thought to be important. 1) Density of initiator sites on the surface. Measures taken were synthesizing of a new polymer, DC15, with fivefold less density of iniferter sites to prevent cross-linking between neighbouring iniferter sites. 2) Creating a two-component iniferter system with radical carriers in solution to prevent unwanted cross-linking between neighbouring initiator sites[10]. 3) Wetness of the surface. Using ethanol as and mixtures of ethanol and water as solvent and incubating samples in monomer solution > 72 h prior to UV-irradiation should both increase availability of monomers to the iniferter surface. 4)Intensity of the UV-lamp.The distance from the lamp to the samples was minimized and the flow of the water coolant was decreased in order to maximize intensity.
5) Higher levels of dissolved oxygen in ethanol. Extra careful degassing and saturating of monomer solution with nitrogen was performed to prevent oxygen from dissolving. 6) Concentration of acrylamide in monomer solution.The concentration of monomer was doubled to have enough monomers in solution.

Taking these measures, reproducibility was achieved both on DC15 and PVBD surfaces. This suggests that the proximity of adjacent benzyls is of less importance for the successful photopolymerization. This leaves the last four alternatives listed above. At present there is no indication which the crucial parameter is or if it is a combination of parameters. The guess though is that the intensity of the UV-lamp is the important factor because no intensitymeter has been used to measure the intensity at the surface of the samples. This equipment is expensive. It would be relatively easy to determine the important parameter/s, however time-consuming.

Given that the substrate polymer, PVBD or DC15 spreads out on the flipside of the crystals, which is always the case when drop-coating, heat as a polymerization initiator is excluded in view of the fact that the backside of successfully photopolymerized samples are hydrophilic on the transparent quartz-edge, but not on the gold, which effectively shades the gold surface. Furthermore, the Pyrex cut-off glass is cold after 60 min of exposure.

In the literature it is shown that the method applied in this study is controllable in the sense that a linear growth of polymer is observed. [9] This way of measuring demands a different experimental set-up and has not been a priority. However, some support for the controllable reaction is seen in Appendix A. When the UV-light is switched on, a linear decrease in the resonance frequency is seen, when the UV-lamp is turned off, the frequency is constant, only to linearly decrease and stop again. However, the shift has not been reproducible and is only ca 80 Hz, and has not been verified by a hydrophilicity test.

In any case, with current parameter settings it seems the method can give acceptable scattering (seeTable 4.8) making comparison possible of different samples.

It is further possible to estimate the thickness of the polymer layer, by substituting Δm in Sauerbrey for $\rho_{gel} \cdot A \cdot \Delta d$ yields $\Delta d = -\frac{\Delta f \left(\rho_q \mu_q\right)^{\frac{1}{2}}}{2 f_0^{\,2} \rho_{gel}}$ (5.1), thus estimating ρ_{gel} can give the thickness of the polymer layer. Since most mass is made of water a guess would be that ρ_{gel} is close to 1 g/cm^3. Suppose the fundamental mode frequency of the crystal is 10 MHz and the shift 1500 Hz. This would give a thickness of ~70 nm. The dependence of the polymer layer thickness to ρ_{gel} is then y = 662,54 x^{-1} for a shift of 1500 Hz. Changing the density from 1,0 to 1,1 gm^{-3} results in a change of thickness by 9 %. A determination of the polymer layer thickness can thus give the density for the matrix.

The diameter of hemoglobin is 5.5 nm[27], so in theory a gel matrix of 70 nm should hold 12 monolayers of hemoglobin, the real number though is obviously much less, but it hints the enormous potential of this technique.

In order to immobilize proteins into a polymer matrix, the EDC/NHS coupling can be used. This coupling uses caroxylate groups which had to be created. To accomplish this, acrylic acid (seeAppendix B for structure), was copolymerized to the acrylamide polymer matrix by adding 10 % acrylic acid to the acrylamide monomer solution. Acrylic acid is also a vinyl and susceptible to photopolymerizaion as acrylamide, and so the iniferter method again shows its strength. The presence of copolymerized acrylic acid is shown by Figure 4.9 using the QCM. The coupling reaction is outlined in Figure 2.2. When activating the acidic copolymer with EDC/NHS, two things happen. A positive frequency shift is expected since activation means loosing charge of polymer, the gel retracts and consequently less water is able to resonate together with the gel. On the other hand the gel is loaded with NHS-groups which would give rise to a negative shift. Obviously the retraction effect is greater than the attachment of NHS to the gel matrix (see Figure 4.12). When the protein solution is introduced, a decrease in frequency is to be attained, because of the coupling of the protein. However if the pH of the protein solution is lower than that of the running buffer this counteracts the negative shift of the binding of the protein. The degree of this effect should decrease for higher pH-values. The sign for maximum expansion of the gel would be a zero or close-to-zero frequency shift effect when the protein buffer passes. To calculate the shift due to protein binding, one has to compare the frequencies before and after the protein plug, or rather after deactivation of NHS and removal of unspecifically bound material by ethanolamine. This behaviour is not optimal. In order to increase availability for the protein to the gel, the pH of the protein solution should be higher than that of the running buffer. In this way, the gel will expand more. Regardless the protein, the pH of the protein buffer should not be too close to the pK_a of the matrix since it gives poor reproducibility, less electrostatic interaction with the protein and sub-optimal steric availability.This has not been the case for the experiment outlined in Figure 4.12. This is probably why the the negative shift of the antibody detection in Figure 4.13 is very low, about 10 Hz.

It is important to determine the pK_a for each gel matrix, since this may vary from gel to gel. K_a is also dependent on temperature, and maybe more important pressure. Care should therefore be taken to use the same flow rate when performing the pH gradient to produce the pKa as when immobilizing proteins. It is important to prepare pH-solutions with accurate values since a small deviation near the pKa can result in a spread in its estimation.

Furthermore, the measuring points should be concentrated near the pK_a, in order to get as close as possible to the real pK_a.

6 Conclusions

- The method used to synthesize and purify substrate iniferter polymers is highly efficient with high yields of product.
- Drop-coating can be used instead of spin-coating as coating method.
- Crucial for reproducible polymerization is one or several of the following parameters: sufficiently high intensity of the UV-lamp, wetness of the sample surface, low levels of dissolved oxygen in solvent, high enough (1M) concentration of acrylamide in monomer solution.
- The polymerization is UV-controlled and not caused by heat.
- The photopolymerization can give fairly reproducible layers with respect to mass.
- Regardless the protein, the pH of the protein buffer should not be too close to the pK_a of the matrix since it gives poor reproducibility, less electrostatic interaction with the protein and sub-optimal steric availability. Choosing a protein with a high pI is favourable, since it is possible to charge it more at a pH far above the pK_a of the gel matrix.

7 Future work

It should in principle be possible to measure the thickness of the polyacrylamide layer with ellipsometry. For this the refractive index of the polymer has to be set. A good guess would be around 1.3 directly after polymerization since it is assumed to contain very much water. In order get good curve-fittings for polyacrylamide, a first layer of substrate polymer, DC15 or PVBD, should be measured in order to obtain thickness and refractive index. When creating the model for polyacrylamide, these properties can be set constant for the substrate polymer when measuring on the very same sample for physical properties for the polyacrylamide layer.

The thickness of a substrate polymer and possibly a polymer matrix layer can be determined directly from the frequency shift. The density of the substrate polymers could be determined according to $\rho_{sp} = -\frac{\Delta f \left(\rho_q \mu_q\right)^{\frac{1}{2}}}{2 f_0^{\,2} \Delta d}$. The frequency has to be measured before and after addition of substrate polymer. This demands that the crystal are mounted into a conducting frame. The only practical problem that has to be solved is to spin-coat on a mounted crystal. For ellipsometry measurement, the crystal can be detached from the frame and measured.

For the immobilization of proteins, it would be of interest to examine the optimization of protein loading capacity, which would include determination of an optimal thickness of the copolymer. It has to be shown that more protein can be loaded into the polymer matrix than onto a conventional monolayer. This could perhaps be done by immobilizing streptavidin followed by subsequent saturation with biotinylated derivatives. A comparison of the responses between the two types of surfaces would show proof of concept.

To continue the MIP-project, the established iniferter photopolymerization method offers the perfect means for doing so. Water should be used as solvent since bis-acrylamide is hard to dissolve in any other solvent.

8 Acknowledgements

I wish to thank Henrik Anderson for the opportunity to do my degree project for Attana and for excellent supervising, I thank my technical supervisor Ulf Lindberg at Solid State Electronics, Uppsala University, for many fruitful discussions and supervision of this report. Thanks to Olof Ramström, Royal Institute for Technology, for a considerable amount of expertise in the field of organic chemistry. Thank you Peter Lindberg for being the scientific reviewer of this report.

Thank you very much Ulrik Gelius for lending yourself to the ESCA experiments, Karin Berggren for introducing me to the project, Mats Jönsson, Hui Yu and Anabel Leroux for assistance in the labs.

I thank the Swedish Research Council for financial support.

9 References

[1] Viitala, T. "What is a quartz crystal microbalance – qcm." http://www.pharmaceutical-int.com/article.asp?pubID=13&catID=1003&artID=2169 (16 Nov.2005).
[2] Eggins, B.R., *Chemical Sensors and Biosensors*, 199-211 (Wiley, Chichester, England, 1999)
[3] Gizeli, E. & Lowe, C.R., *Biomolecular Sensors*, 291-299 (Taylor & Francis, London, UK, 2002)
[4] Karin Berggren, A gel based QCM biosensor-Investigation of deposition, *12 Credits Research Training Period Report at Uppsala University* (2005).
[5] Wikipedia http://de.wikipedia.org/wiki/Atom_Transfer_Radical_Polymerization (16 Nov.2005).
[6] Huang, X., Doneski, L. J. & Wirth, M.J., Surface-confined living radical polymerization for coatings in capillary electrophoresis. *Anal. Chem.* **70**, 4023-4029 (1998).
[7] Digital Library and Archives, Controlled/"living" free radical polymerizations: http://scholar.lib.vt.edu/theses/available/etd-04192001-153328/unrestricted/9_Chapter_1.pdf (16Nov.2005).
[8] Thomas, D.B., Sumerlin, B.S., Lowe, A.B. & McCormick, C.L., Conditions for facile, controlled RAFT polymerization of acrylamide in water. *Macromolecules* **36**, 1436-1439 (2003).
[9] Nakayama, Y. & Matsuda, T., In situ observation of dithiocarbamate-based surface photograft copolymerization using quartz crystal microbalance. *Macromolecules* **32**, 5405-5410 (1999).
[10] Otsu, T. & Matsunaga, T., Doi, T. & Matsumoto, A., Features of living radical polymerization of vinyl monomers in homogeneous system using N,N-diethyldithiocarbamate derivatives as photoiniferters. *Eur. Polym. J.*, **31**, 67-78 (1995).
[11] Johnsson, B., Löfås, S. & Linquist, G., Immobilization of proteins to a carboxymethyldextran-modified gold surface for biospecific interaction analysis in surface plasmon resonance sensors. *Analytical Biochemistry* **198**, 268-277 (1991).
[12] Chan, E.C. & Ho, P.C., Preparation and characterization of immunogens for antibody production against metanephrine and normetanephrine. *J. Immunol. Methods*, **266**, 143-154 (2002).
[13] Kara P., Erdem, A., Girousi, S. & Ozsoz, M., Electrochemical detection of enzyme labeled DNA based on disposable pencil graphite electrode., *J. Pharm. Biomed. Anal.* **38,** 195-195 (2005).
[14] Fung, Y.S. & Wong, Y.Y., Self-assembled monolayers as the coating in a quartz piezoelectric crystal immunosensor to detect Salmonella in aqueous solution. *Anal. Chem.* **73**, 5302-5309 (2001).
[15] Howell, S., Kenmore, M., Kirkland, M. & Badley R.A., High-density immobilization of an antibody fragment to a carboxymethylated dextran-linked biosensor surface. *J. Mol. Recognit.* **11**, 200-203 (1998).
[16] Lange, K., Bender, F., Voigt, A., Gao, H. & Rappt, M., A surface acoustic wave biosensor concept with low flow cell volumes for label-free detection. *Anal. Chem.* **75**, 5561-5566 (2003).
[17] Abbas, A.K., & Lichtman, A.H., *Cellular and Molecular Immunology*, 45-47 (Elsevier Science, Philadelphia, USA, 2000).
[18] Mosbach, K. &Ramström, O.,The emerging technique of molecular imprinting and its future impact on biotechnology. *Nature Biotechnology* **14**, 163-170 (1996).
[19] Liao, J.-L., Wang, Y. & Hjertén, S., A novel support with artificially created recognition for the selective removal of proteins and for affinity chromatography. *Chromatographia* **42**, 259-262 (1996).
[20] S. Hjertén, *et al*. Gels mimicking antibodies in their selective recognition of proteins. *Chromatographia* **44**, 227-234 (1997)
[21] Hibert, C., "Optical profiler Veeco Wyko NT1100" http://cmi.epfl.ch/metrology/Wyko_NT1100-v03.htm (16 Nov.2005).
[22] "Basic principles" http://www.jobinyvon.com/usadivisions/TFilms/basicellip.htm 16 Nov.2005).
[23] Moulder, J.F., Stickle, W.F., Sobol, P.E., & Bomben, K.D., *Handbook of X-ray Photoelectron Spectroscopy*, firstpage-lastpage (Perklin-Elmer Corporation Physical Electronics Division, City,country, 1992).
[24] Beamson, G. & Briggs, D., *High Resolution XPS of Organic Polymers – The Scienta ESCA300 Database*, firstpage-lastpage (John Wiley & Sons, City, Country, 1992).
[25] Guan, Z. & DeSimone, J.M., Fluorocarbon-based heterophase polymeric materials. 1. Block copolymer surfactants for carbon dioxide applications, *Macromolecules* **27**, 5527-5532 (1994).
[26] de Boer, B., Simon, H.K., Werts, M.P.L., van der Vegte, E.W. & Hadziioannou, G., "Living" free radical photopolymerization initiated from surface-grafted iniferter monolayers. *Macromolecules* **33**, 349-356 (2000).
27 Natzke, L., 1998 "Hemoglobin" http://biology.kenyon.edu/BMB/Chime/Lisa/FRAMES/hemetext.htm (17 Nov.2005)

Appendix A

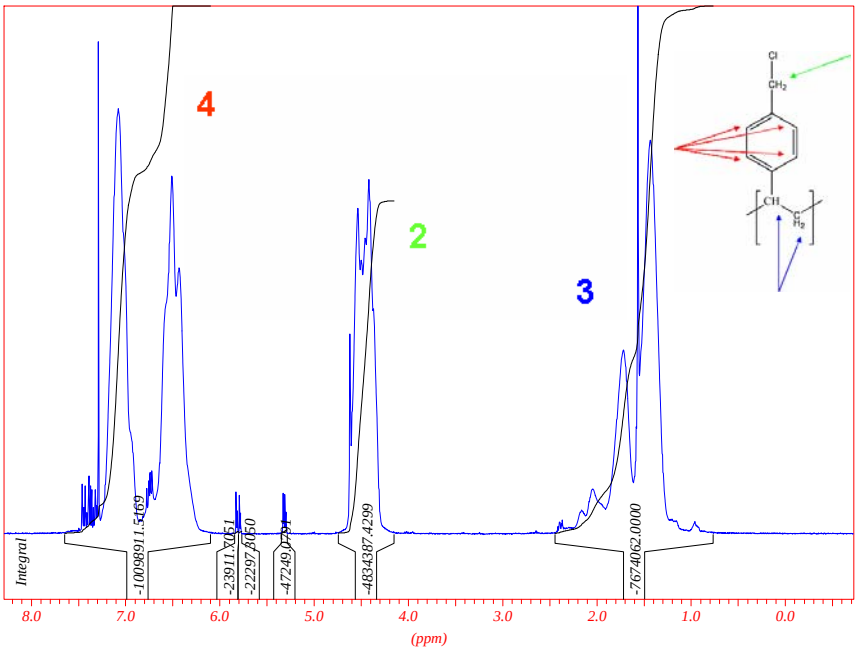

NMR-spectrum of PVBC. The ratios of the integrals are 4:2:3.

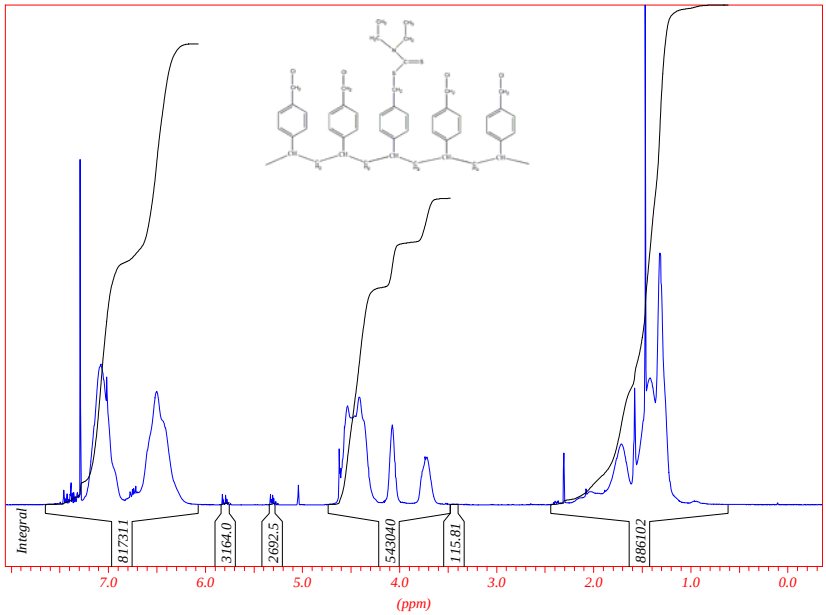

NMR spectrum of DC15. The ratios of the integrals are 20:13.3:21.7.

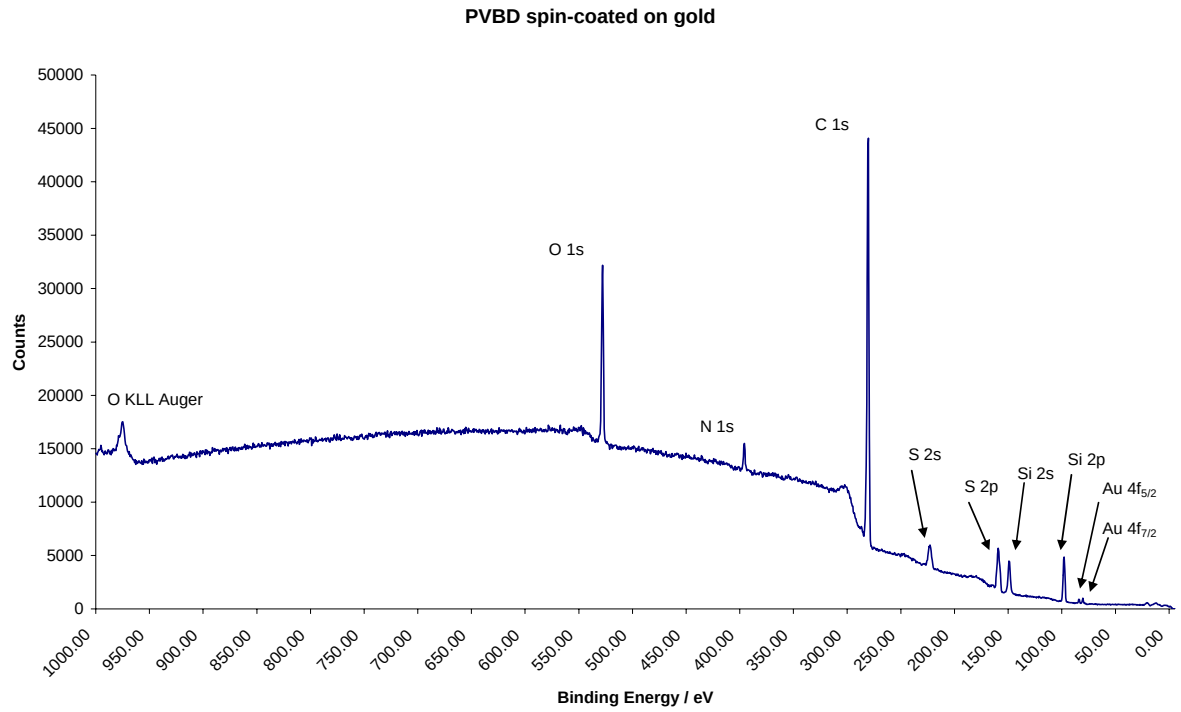

Spectrogram of spin-coated PVBD on gold substrate. Y-axis, number of counts; x-axis, binding energy in electron volts. The nitrogen 1s and sulphur 2s and 2p peaks are visible at ca 400, 225 and 155 eV respectively. Elements with higher Z have higher binding energy for electrons in the s-orbitals. Peaks from electrons in s-orbitals are seen left to the p-orbitals. To the very left in the spectrogram is a peak stemming from Auger electrons originating from the L orbital. The elevated base line to the left of the carbon 1s peak is due to inelastic scattering of carbon 1s electrons, a small shift is also seen to the left of the oxygen 1s peak. Hence, these electrons origin from deeper beneath the surface and hints that carbon and oxygen are present in the bulk. Detector is positioned at 90° relative to the sample surface.

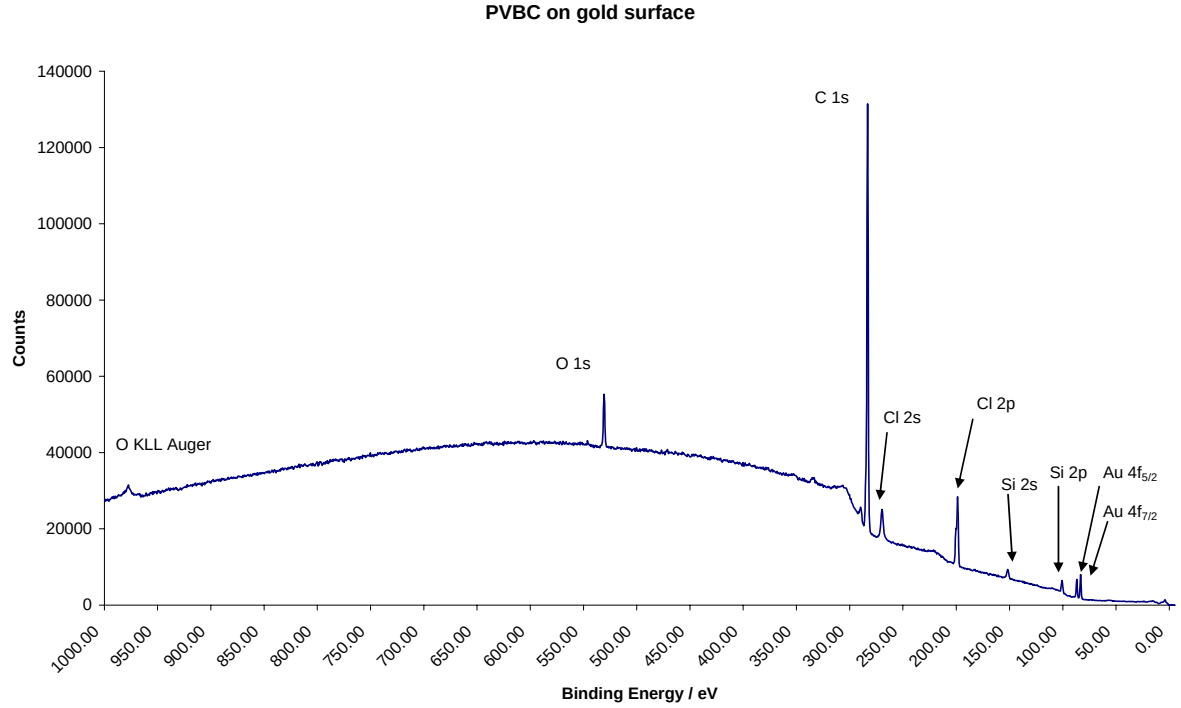

Spectrogram of spin-coated PVBC on gold substrate. No nitrogen or sulphur peaks are visible; instead chlorine 2s and 2p peaks appear at about 275 and 200 eV respectively.

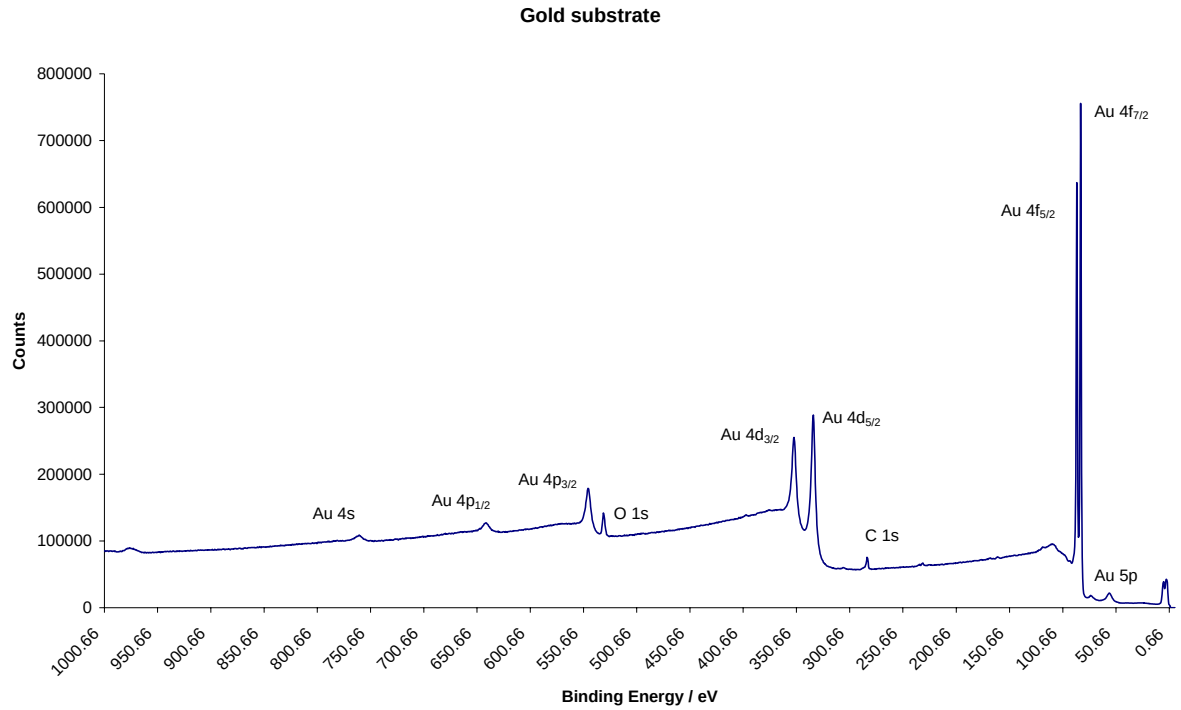

Gold substrate reference. Minor contaminations of carbon and oxygen.

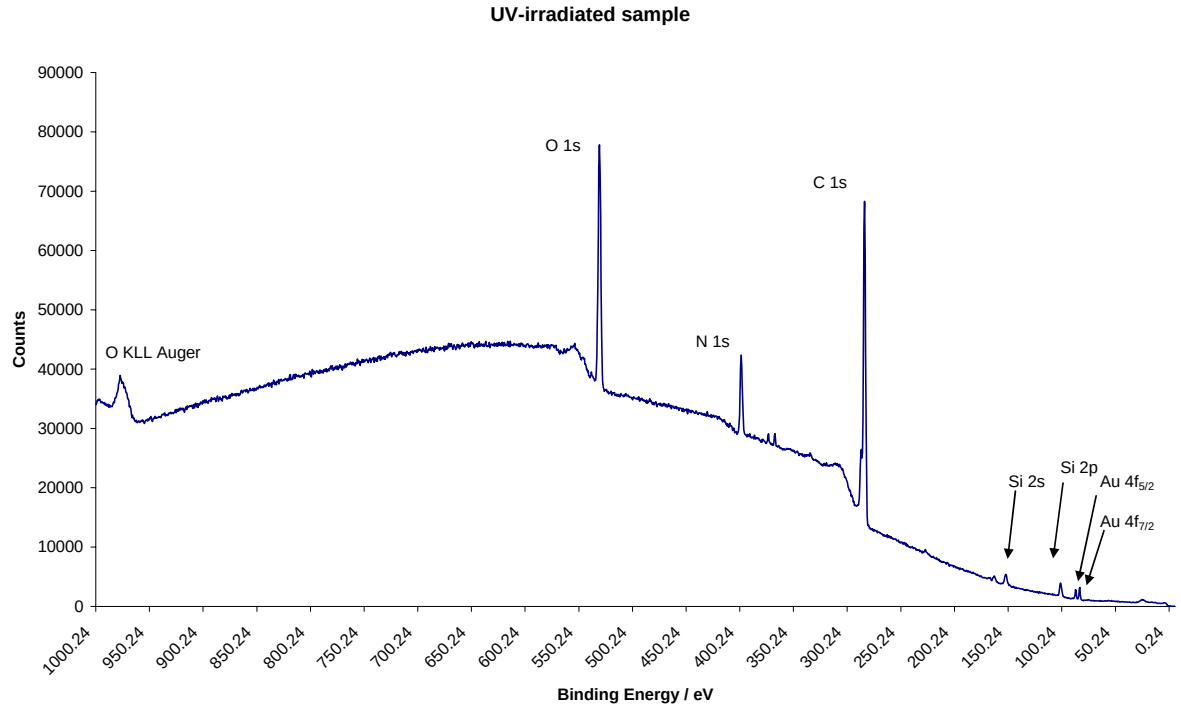

Spectrogram of UV-irradiated PVBD sample in 0.5 M acrylamide monomer solution. Irradiation time is 60 min. The oxygen density is higher relative the carbon. No or little sulphur is detected.

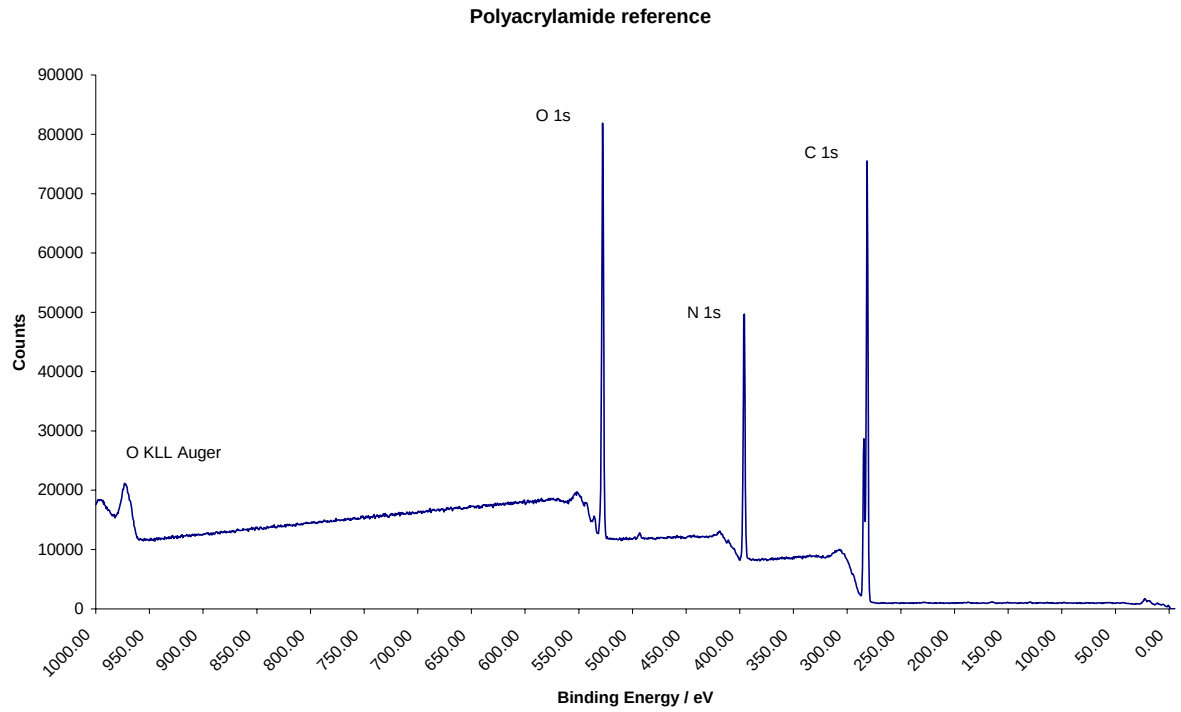

Spectrogram of an APS initiated pure polyacrylamide reference. Detector is positioned at a 30° angle to the sample.

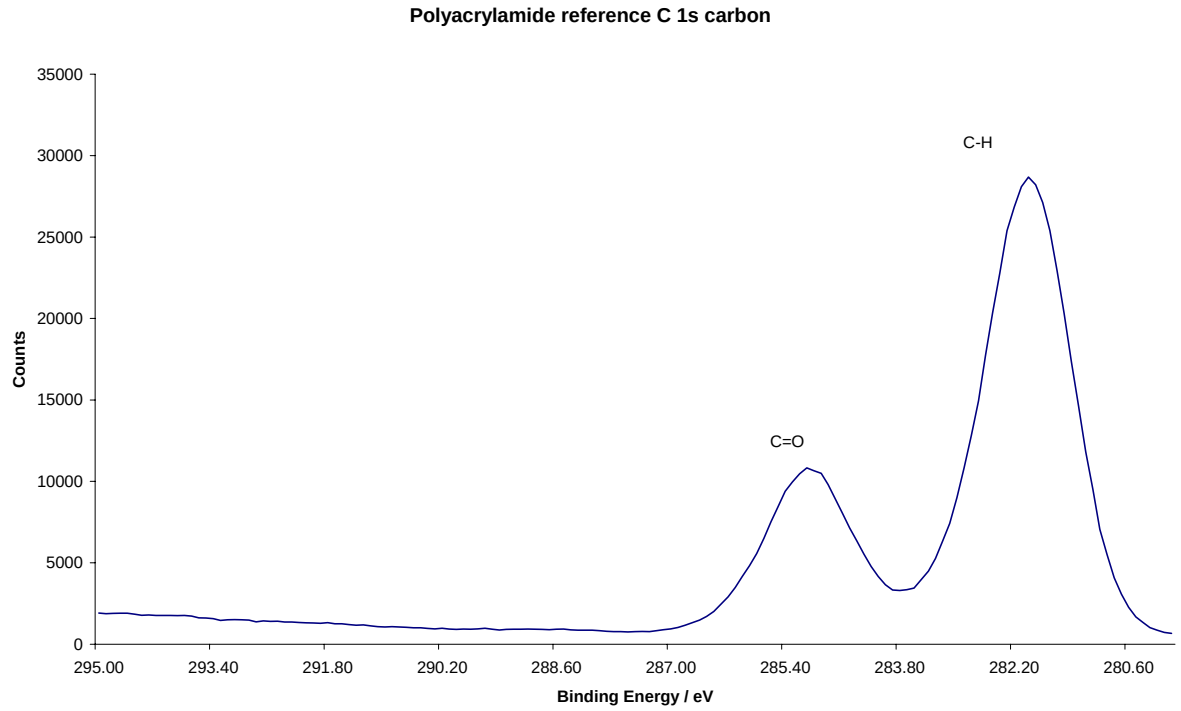

Spectrogram of the C 1s carbon of the polyacrylamide reference sample. The double-bound oxidized carbon is detected.

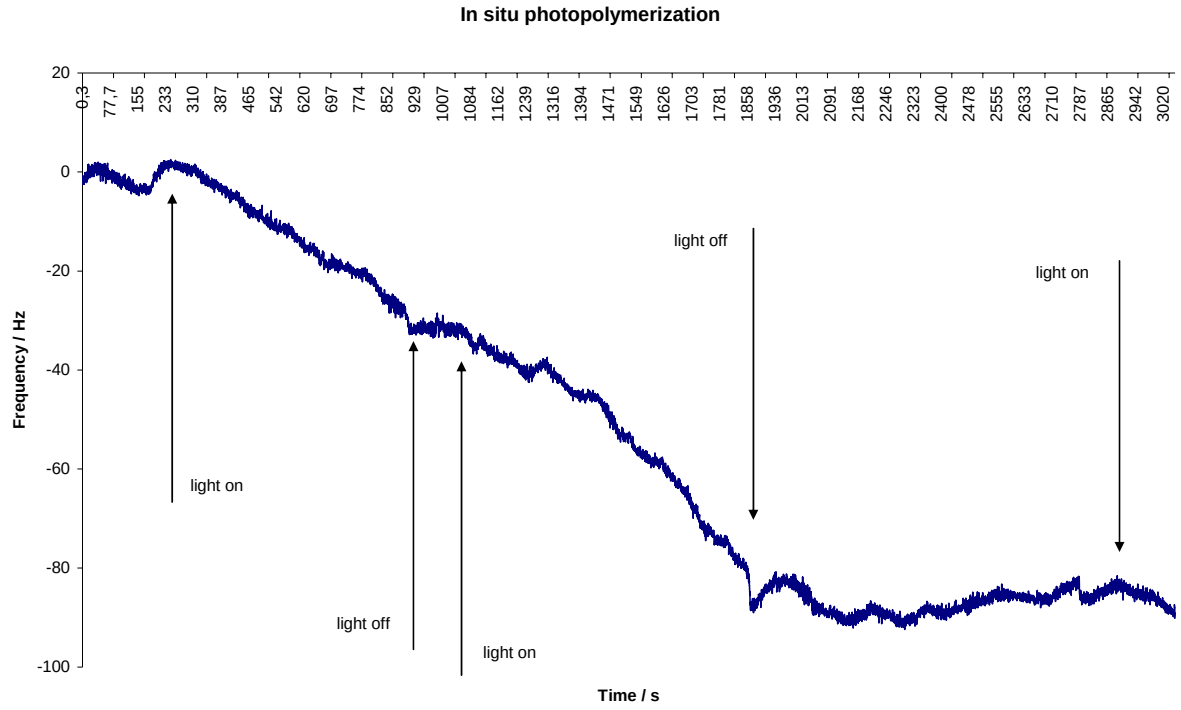

In situ experiment where QCM measurements were performed during the photopolymerization. A linear shift can be seen when the UV-lamp is on, but no shift when it is turned off.

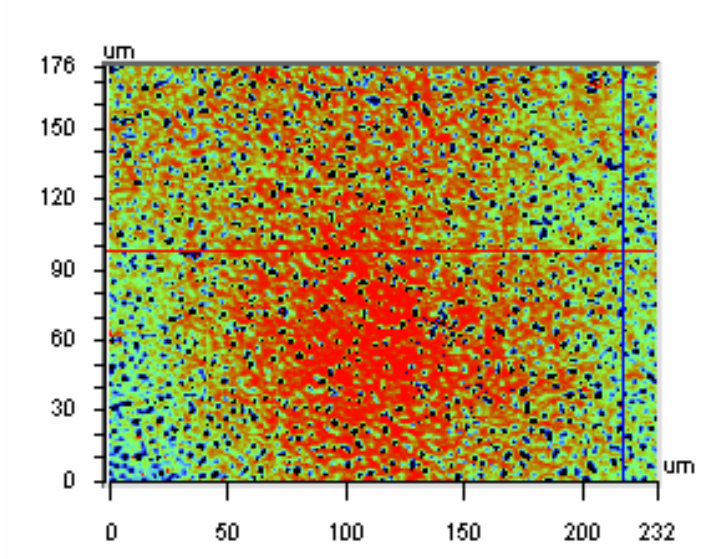

Surface profiling of spin-coated PVBD using THF as a solvent. Red color denotes higher areas, blue lower and green average height areas. The red horizontal and blue vertical lines are profiles that are depicted in and respectively.

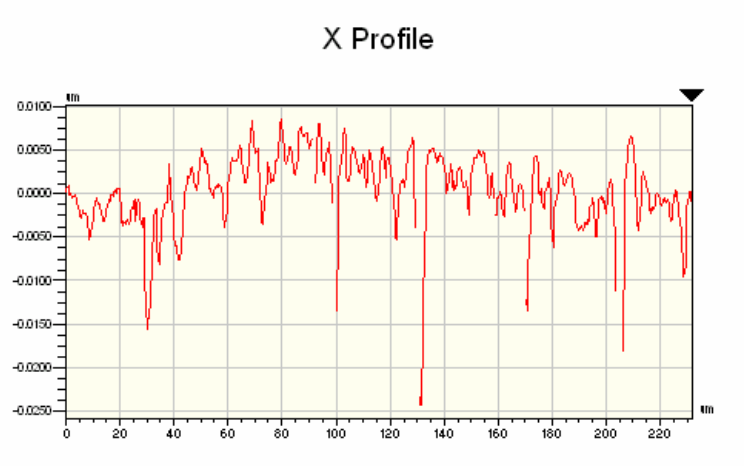

Horizontal profile of surface spin-coated PVBD sample. Scales are in µm. The highest peak is 0.01 µm and deepest valley 0.02 µm. Largest difference is 30 nm. RMS is 0 µm.

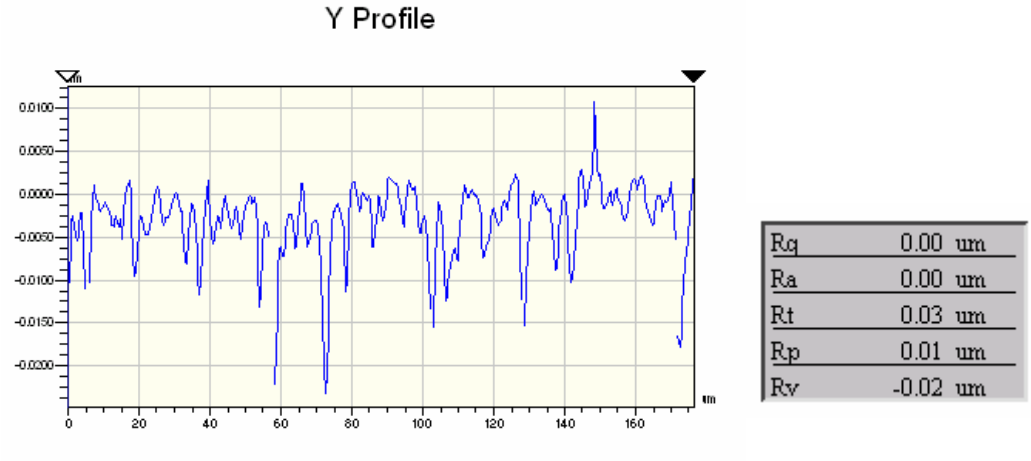

Vertical profile profile of surface spin-coated PVBD sample. Scales are in µm. The highest peak is 0.01 µm and deepest valley 0.02 µm. Largest difference is 30 nm. RMS is 0 µm.

Appendix B

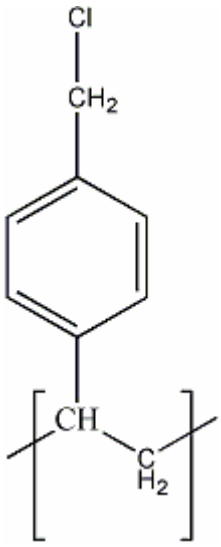

PVBC unit

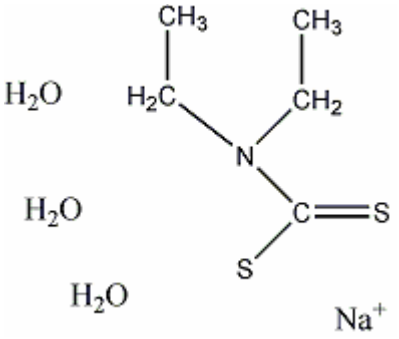

NaDC Trihydrate

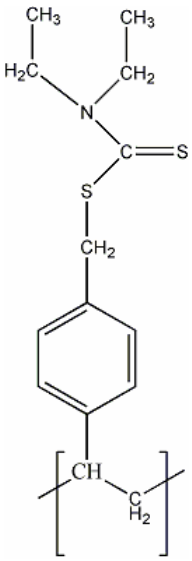

PVBD unit

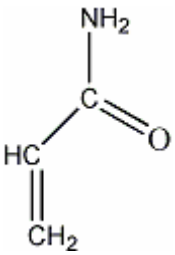

Acrylamide monomer

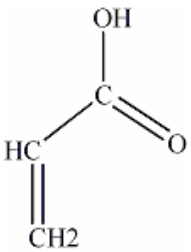

Acrylic acid monomer

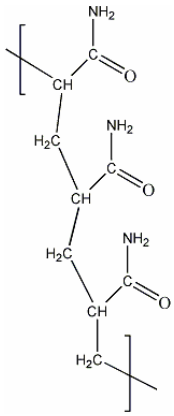

Polyacrylamide chain